CHAPTER 14

PLUME WINTER SCENARIO FOR BIOSPHERE CATASTROPHE: THE PERMO-TRIASSIC BOUNDARY CASE

YUKIO ISOZAKI

Department of Earth Science and Astronomy, The University of Tokyo, Komaba, Meguro, Tokyo 153-8902 Japan;
E-mail: isozaki@chianti.c.u-tokyo.ac.jp

Abstract
The Permo-Triassic boundary (P-TB) interval is unique in having experienced three unusual geologic phenomena on a global scale that had never occurred in the rest of the Phanerozoic, viz., 1) the greatest mass extinction, 2) development of superanoxia (nearly 20 million year-long anoxia), and 3) initial breakup of the supercontinent Pangea. The so-called end-Paleozoic mass extinction was double-phased, one at the Guadalupian-Lopingian boundary (G-LB; ca. 260 Ma) and the other at the Changhsingian/Induan boundary (P-TB *sensu stricto*; ca. 252 Ma). The coincidence in timing between the G-LB mass extinction, the onset of superanoxia, and the probable initial rifting of Pangea strongly suggests their causal link. This article reviews current understanding of the end-Paleozoic event, and proposes a possible scenario to explain these three unique geological phenomena in a cause–effect context. Violent volcanism is favored by many on the basis of the apparent coincidence in timing between the two Late Permian mass extinctions and the volcanism of continental flood basalts (CFB). However, the only available material-based evidence for putative violent volcanism is the felsic tuffs in the Upper Permian in South China and Japan that appear inconsistent with the CFB link. The end-Paleozoic global environmental change was likely triggered by the episodic activity of a mantle plume, not through basaltic but rhyo-dacitic volcanism. The felsic nature of the volcanism suggests not only highly explosive eruption but also extensive delivery of air-borne ash. Alkaline magmatism derived directly from a mantle plume, may have played an important role both in the G-LB and P-TB extinction-relevant environmental turmoils. The "Plume Winter" scenario is proposed here to explain the unique geological phenomena of the end-Paleozoic event. When a plume head hits the bottom of a pre-existing continental lithosphere, alkaline volcanism of felsic to intermediate composition, often accompanying kimberlite/carbonatite, occurs in a highly explosive manner prior to a voluminous CFB eruption in a later stage. The violent volcanism directly causes 1) extensive ash fall, 2) formation of a dust/aerosol-screen in the stratosphere, and 3) acid rain, and these are followed by severe destruction of the photosynthesis-supported global food web both on land and in sea through 4) less insolation and 5) low temperature. A sharp decline or cessation of the primary production may have triggered cascaded extinctions of marine and terrestrial

D. A. Yuen et al. (eds.), Superplumes, 409–440.
© 2007 *Springer.*

heterotrophic animals. In the aftermath, increase in atmospheric CO_2 by volcanism drives global warming, prolonged anoxia, and delayed biotic recovery. "Plume Winter" initiated by the uprising African superplume may have caused the end-Paleozoic double-phased mass extinction and the superanoxia. The G-LB event appears to have been more important than that at P-TB, because everything geologically significant started at that time, viz. the initial breakup of Pangea, mass extinction, and superanoxia. This is also supported by the remarkable turning point of the Phanerozoic in the global sea level, initial $^{87}Sr/^{86}Sr$ ratio of seawater, and geomagnetic field behavior. The major re-organization of the mantle plume structure from the Pacific to the Atlantic regimes corresponds to the largest turning point in the Phanerozoic history of life from the Paleozoic to the Mesozoic-Modern regime.

1 INTRODUCTION

In the last one ninth of Earth's history, the Phanerozoic (ca. 542 million years), five major mass extinction events occurred at the end-Ordovician, Late Devonian, end-Permian, end-Triassic, and end-Cretaceous (Sepkoski, 1984; Hallam and Wignall, 1997). As each event was unique in character, it seems unlikely that there was only one common cause that drove all the five extinction events. An extraterrestrial cause has only been proved reliably for the end-Cretaceous (K-T boundary) event (Alvarez, 1997). Although a similar K-T boundary-style impact was claimed for the Late Devonian, end-Permian, and end-Triassic events, none of these has been supported by convincing evidence. This definitely suggests that there were other causes, in particular those related to terrestrial processes.

Among the big five mass extinctions, the end-Permian (=Permo-Triassic boundary or P-TB; ca. 252 Ma) event is outstanding because it marks the greatest divide in Phanerozoic biosphere history, i.e., the irreversible change from the Paleozoic to the Mesozoic-Modern regime (Sepkoski, 1984). We can recognize three distinct global geologic phenomena that occurred uniquely at the P-TB time; i.e., 1) the largest mass extinction, 2) superanoxia, and 3) the initial breakup of the Pangea supercontinent. All these three geological events are unique to the P-TB as they have never been recorded as having happened in the rest of the Phanerozoic. Judging from their global nature, such uniqueness potentially suggests that these three phenomena occurred at the same time not by accident but in a tight cause–effect link(s), probably through terrestrial processes.

This chapter reviews the current understanding of the P-TB event, focusing on the above-mentioned three distinct and unusual geological phenomena, and discusses their possible cause–effect link in a new volcanism-triggered scenario named the "Plume Winter". In contrast to the Phanerozoic era, Precambrian time appears to provide little or no information on mass extinctions, owing to the scarcity of the fossil record; however, the current approach, assuming Earth-bound and mantle plume-related mechanisms of mass extinction, may open a new window into the *Terra incognita*.

2 P-TB EVENT

The greatest mass extinction in the Phanerozoic was at the Permo-Triassic boundary (P-TB), at a time when many marine and terrestrial biotas were terminated (e.g., Sepkoski, 1984; Erwin, 1993; Benton, 1985; Visscher et al., 1996). Despite the variety of hypotheses and ideas proposed in the last 100 years by many researchers, the ultimate cause of the P-TB mass extinction has not yet been identified (e.g., Hallam and Wignall, 1997; Erwin et al., 2002; Bottjer, 2004). Following research on the K-T boundary, similar evidence for an extraterrestrial impact such as an Ir anomaly was claimed for the P-TB event, but all efforts to produce similar data failed totally (Clark et al., 1986; Zhou and Kyte, 1988). Likewise, a recently reported ^{3}He anomaly from the P-TB (Becker et al., 2001) is not convincing because of poor analytical procedures that violated the double-blind test protocol (Farley et al., 2005). In addition, an analyzed sample from Japan was obviously taken not from the P-TB horizon but from the Upper Permian interval (Isozaki, 2001). Even concerning a possible *bona fide* P-TB sample from South China, Kaiho et al. (2001) reported more data to support an extraterrestrial impact but these are criticized to be equivocal by Koeberl et al. (2002). The notion that the "Bedout" impact off Western Australia caused the P-TB extinction (Becker et al., 2004) was immediately questioned by Wignall et al. (2004) and Renne et al. (2004). A P-TB impact in the southern hemisphere sounds unrealistic because Paleozoic radiolarians became completely extinct in the northern hemisphere at the P-TB, whereas they survived solely in the southern hemisphere off New Zealand (Takemura et al., 2003). Judging from such long-term intense efforts in search of extraterrestrial signatures and from the barren results so far, it seems likely at present that there is no convincing evidence to support extraterrestrial impact at the P-TB.

By assuming no planetary impact, we may look for a more reasonable cause for the P-TB catastrophe within our own planet. Besides the greatest mass extinction in the Phanerozoic, the P-TB interval is characterized by two other unusual geologic events of global significance, i.e., the development of extraordinarily long-lasting oxygen-depleted condition called superanoxia (Isozaki, 1994, 1997), and the initial breakup of the supercontinent Pangea. As these two events never occurred together at any other time in the Phanerozoic except for at the P-TB, their apparent coincidence in timing with the greatest mass extinction of the Phanerozoic strongly suggests a potential cause–effect relationship (Fig. 1). Thus the ultimate cause of the P-TB event may be better sought by establishing possible viable link between these three unusual global phenomena of the Phanerozoic.

2.1 Extinction

The P-TB mass extinction has long been regarded as the most outstanding biological turnover event in the Phanerozoic, when nearly 90% of marine invertebrate species and a comparable diversity of land biota were terminated (e.g., Sepkoski, 1984; Labandeira and Sepkoski, 1992; Erwin, 1993; Benton, 1985; Visscher et al., 1996; Hallam and Wignall, 1997; Fig. 2a). The severity of the mass extinction is

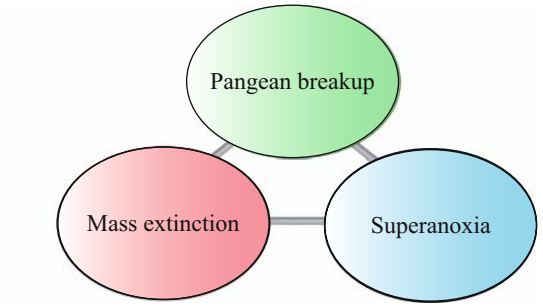


Figure 1. Schematic diagram showing three unusual geologic phenomena of global context that make the Permian-Triassic boundary (P-TB) event unique in the Phanerozoic. The main goal of the current P-TB study is to establish possible cause–effect relationships among these three global geologic phenomena unique to the P-TB.

biostratigraphically documented in various P-TB sections around Pangea including South China (Zhao et al., 1981; Yin, 1996; Yin et al., 2001), the Tethyan domain of the Middle East and Europe (e.g., Iranian-Japanese Research Group, 1981; Pakistani-Japanese Research Group, 1985; Holser and Schoenlaub, 1991; Cirilli et al., 1998), Laurentia of Greenland (e.g., Looy et al., 2001), and South Africa plus Australia in Gondwana (e.g., MacLeod et al., 2000; Retallack et al., 2003; Thomas et al., 2004). In particular in the Global Stratotype Section and Point (GSSP) of the P-TB at Meishan, South China, the sharp termination of more than 150 species is well-documented (Yang et al., 1991; Jin et al., 2000). In addition, even in the middle of the superocean Panthalassa, the extinction of Paleozoic radiolarians, fusulines, and rugose corals was detected in mid-oceanic deep-sea chert and shallow marine atoll carbonates (Isozaki, 1994, 1997, 2007; Koike, 1996). Thus the P-TB mass extinction was a global occurrence, affecting both Pangea and Panthalassa from low- to high-latitudes.

The main extinction timing of the P-TB is chronologically constrained at 252.6 Ma by the latest sophisticated dating techniques (Mundil et al., 2004), although the tempo and duration of the main pulse are not yet clarified. In addition, chemostratigraphic analyses have identified a sharp negative shift in stable carbon isotope ratios across the P-TB in almost all P-TB sections across the world (e.g., Holser et al., 1989; Baud et al., 1989; Yin, 1996; Musashi et al., 2001), indicating that the carbon cycle in the ocean-atmosphere was significantly perturbed at the P-TB on a global scale, probably coupled with a change in global bio-productivity. The post-extinction recovery was considerably delayed both in the biodiversity and complexity of the ecosystem compared with other major extinctions of the Phanerozoic (Bottjer, 2004), as clearly demonstrated by low-diversity fauna, a secular change in ichnofabric (Schubert and Bottjer, 1995; Twitchett, 1999) and the development of a "reef gap" (Stanley, 1988).

Recent results suggest that the end-Permian mass extinction was double-phased; the first extinction at the Guadalupian-Lopingian boundary (G-LB, Middle-Upper Permian boundary) and the second at the Lopingian-Induan boundary (P-TB *sensu*

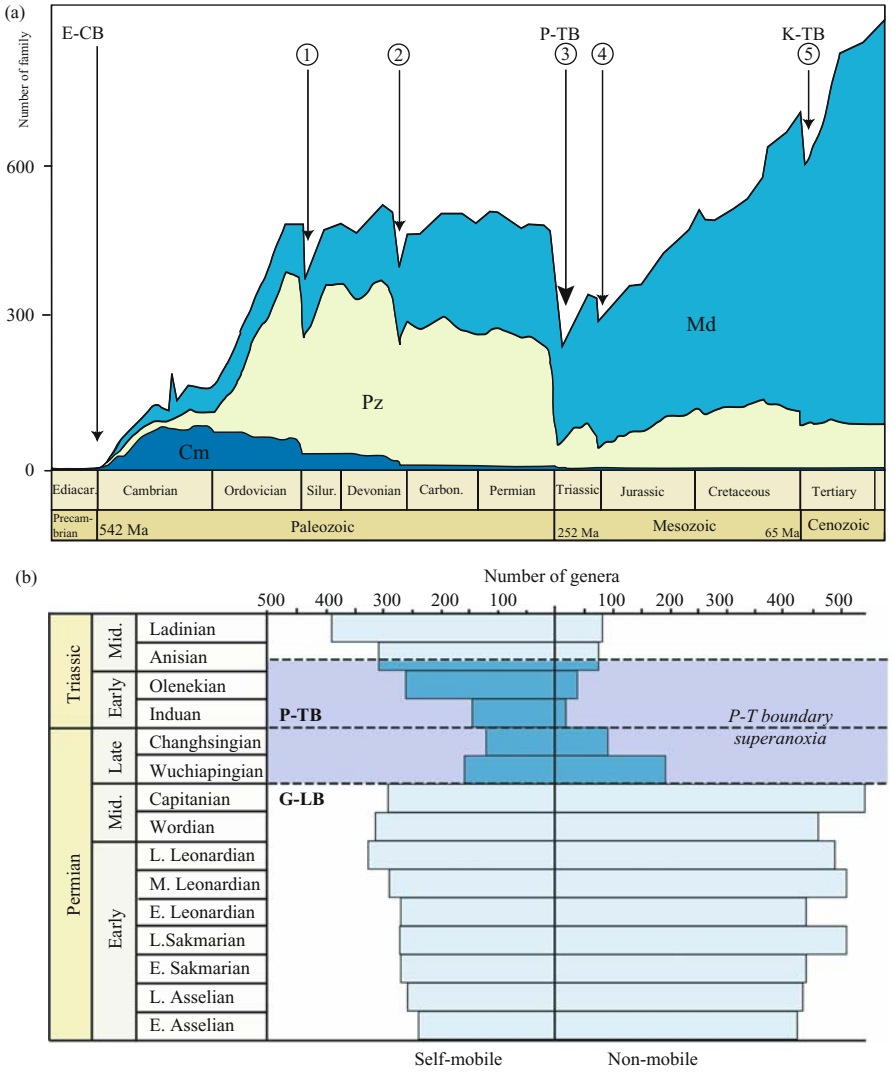


Figure 2. Secular change in biodiversity in the Phanerozoic (A: modified from Sepkoski, 1984) and across the P-TB (B: modified from Knoll et al., 1996). a: The P-TB mass extinction represents the greatest in the Phanerozoic but it is in fact composed of two distinct extinction events; i.e., the Guadalupian-Lopingian boundary (G-LB) event and the Changhsingian/Induan boundary (P-TB *sensu stricto*) event, that occurred in a relatively short time interval less than 10 million years. b: An overall bottleneck pattern in biodiversity is clearly observed across the P-TB in general, however, the most severe extinction occurred first at the G-LB, preferentially terminating bottom-dwellers (sessile benthos) with passive respiratory systems, prior to the P-TB. The prominent end-Paleozoic extinction was a combined consequence of the two distinct extinction events.

stricto). Since Stanley and Yang (1994) and Jin et al. (1994) pointed out the double-phased nature of the end-Permian extinction based on data from South China, the significance of the G-LB extinction event has become more apparent (Fig. 2b). Biostratigraphical research on coeval mid-oceanic deep-sea cherts and shallow marine atoll carbonates has confirmed that the double-phased faunal turnover occurred in radiolarians and fusulines in mid-Panthalassa as well as in peri-Pangean shelf sediments (Isozaki, 2007; Ota and Isozaki, 2006). Noteworthy is the same magnitude of extinction (extinction rate nearly 90% at species level) in the two events and a relatively short time interval between them, less than 10 million years. Thus the responsible global environmental change should have also been double-phased to account for the independent two mass extinctions. The devastating diversity-loss of the Paleozoic biota at the P-TB was probably due to the fact that the two large events occurred in a back-to-back manner in a short interval that did not allow enough time for the biosphere to recover to the pre-existing level in the Permian (Stanley and Yang, 1994; Isozaki, 2007). With a long-term viewpoint of Phanerozoic evolutionary history, therefore, the drastic change from the Paleozoic to the Mesozoic-Modern regime most likely started not at the P-TB *per se* but probably at the G-LB, viz. nearly 10 million years earlier than previously believed.

2.2 Superanoxia

Detailed stratigraphical studies of accreted mid-oceanic deep-sea cherts in Japan and British Columbia (Fig. 3a) have demonstrated that a long-term oxygen-depleted condition (oceanic anoxia) occurred in the Late Permian to Middle Triassic (Isozaki, 1994, 1997). This unique geological phenomenon, named superanoxia, lasted for an unusually long period during the Lopingian (Late Permian), Induan-Olenekian (Early Triassic) and early-middle Anisian (Middle Triassic) (Fig. 3b). According to the latest geologic timescale (Gradstein et al., 2004), this superanoxic interval ranged for ca. 20 million years from 260 to 240 Ma.

The secular change in the oceanic redox state was first detected in the sensitive switch of Fe-bearing minerals in deep-sea chert; i.e., hematite in oxic vs. pyrite in reduced conditions, as reflected in chert color (red vs. gray). The symmetrical pattern in redox state across the P-TB was confirmed by various geochemical analyses utilizing rare earth element abundances, Mössbauer spectroscopy, and trace element abundances (Kakuwa, 1996; Kato et al., 2002; Matsuo et al., 2003; Xia et al., 2004). Some sulfur isotope and organic geochemical analyses suggested the existence of a short-term oxic spike within this superanoxic period (Kajiwara et al., 1994; Suzuki et al., 1998), but this idea was later criticized (Wignall and Twitchett, 2002). During the P-TB superanoxia, deep-sea sediments became enriched both in pyrite and organic carbon, suggesting an anoxic and even euxinic condition mostly in the superocean (Isozaki, 1997) except for some areas in the southern hemisphere (Takemura et al., 2003). At the P-TB in the midst of the superanoxia, Paleozoic radiolarians became extinct particularly in the northern hemisphere. As radiolarians were the main representative plankton in the Paleozoic, their extinction most likely led to a major reorganization of the global bio-productivity and marine food web system. These

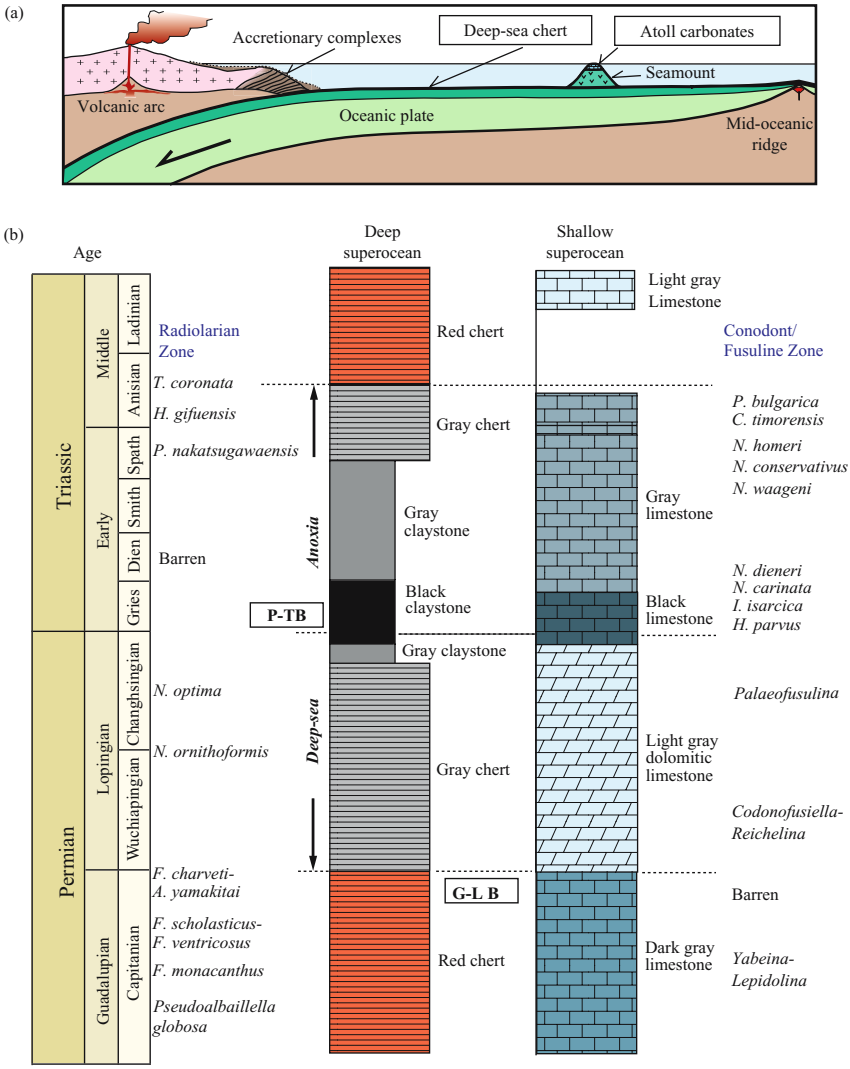


Figure 3. Schematic diagram showing the primary depositional sites of deep-sea pelagic cherts and mid-oceanic atoll carbonates in a simplified ridge-trench transect (a), and the composite stratigraphic columns of the Permian-Triassic deep-sea cherts and shallow-marine paleo-atoll carbonates deposited in the mid-Panthalassa (a: simplified from Isozaki et al., 1990; b: modified from Isozaki, 2007). Pre-Jurassic mid-oceanic records can be obtained solely from ancient oceanic rocks contained in subduction-accretion complexes formed along the ancient active continental margin because all pre-Jurassic seafloors had completely disappeared from the Earth's surface by the successive plate tectonics-driven subduction processes (a). The Jurassic accretionary complex in Japan contains numerous exotic blocks of the Permo-Triassic deep-sea chert and atoll carbonates of mid-oceanic origin, and some retain coherent primary stratigraphy across the G-LB and P-TB (b). These oceanic rocks are biostratigraphically tuned in high resolution by microfossils (fusulines, conodonts, and radiolarians). Three horizons, i.e., G-LB, P-TB, and

relations suggest that the oceanography of Panthalassa was drastically perturbed on a global scale, coupled with large changes in environment and biota *per se*. Such an anomaly in ocean is clearly reflected in the unusual deposition of anachronistic (Precambrian-like) aragonite precipitates during the Early Triassic (e.g., Schubert and Bottjer, 1992; Woods et al., 1999).

The superanoxia probably culminated at the P-TB, because the P-TB interval is centered by a unique, jet black, carbonaceous/pyritiferous siliceous shale (probably of the Griesbachian age; Yamakita et al., 1999) within a deep-sea chert succession (Fig. 3b). Moreover, shallow marine sequences recorded a short-term anoxia in the lowermost Triassic (e.g., Wignall and Hallam, 1992; Grice et al., 2005). These observations indicate that anoxic waters may have originated in the deep-sea in the Late Permian, invaded shallow-sea including continental shelves across the P-TB, and finally retreated to the deep-sea in the early Middle Triassic (Isozaki, 1996, 1997; Fig. 4).

Noteworthy is the timing of onset and disappearance of the superanoxia, because it coincided with major changes in biological diversity in the Late Permian and Middle Triassic (Fig. 3). The superanoxia started at the G-LB when the first mass extinction occurred. In contrast, the superanoxia started to wane in the late Olenekian to early Anisian by showing a fluctuation in redox, and finally it completely disappeared in the middle Anisian. This timing corresponds precisely with that of the full recovery of biodiversity, in particular, the re-appearance of reef complexes after a nearly 10 million-year gap (Stanley, 1988). These coincidences in timing suggest a causal link between the redox change in the superocean and the biodiversity.

2.3 Pangean breakup

Ever since Valentine and Moores (1970) and Schopf (1974) pointed out the sharp correlation between continent distribution pattern and secular change in biotic diversity in the Phanerozoic (amazingly just 5 years after the formulation of modern plate tectonics), the link between solid Earth processes and the biosphere crisis has attracted considerable interests from numerous geologists. Since 2.7 Ga, the formation and breakup of supercontinents have taken place at least 4 or 5 times (e.g., Hoffman, 1991; Dalziel, 1995; Rogers and Santosh, 2004). Late Paleozoic to early Mesozoic Pangea was the only supercontinent that appeared in the Phanerozoic. During the Late Carboniferous, two large continents, Gondwana and Laurasia, merged to form Pangea by closing an intervening ocean that corresponds to the western part of Tethys.

Figure 3. (*Continued*) mid-Anisian, are particularly noteworthy in correlation because synchronous phenomena are observed between the deep-sea chert and shallow marine carbonates. Faunal turnover both at the G-LB and P-TB is clearly detected in the deep-sea chert with radiolarians and in the atoll carbonates with fusulines. These two pulses in biodiversity change indicate that the relevant environmental change were of global in context. The onset of the ca. 20 million year-long deep-sea anoxia (superanoxia; Isozaki, 1994) apparently coincides with the G-LB event, whereas the superanoxia disappeared in the Anisian (Middle Triassic) at the time of full recovery in reef development and in global biodiversity. It is noteworthy that the P-TB event occurred in the climax of the superanoxic period.

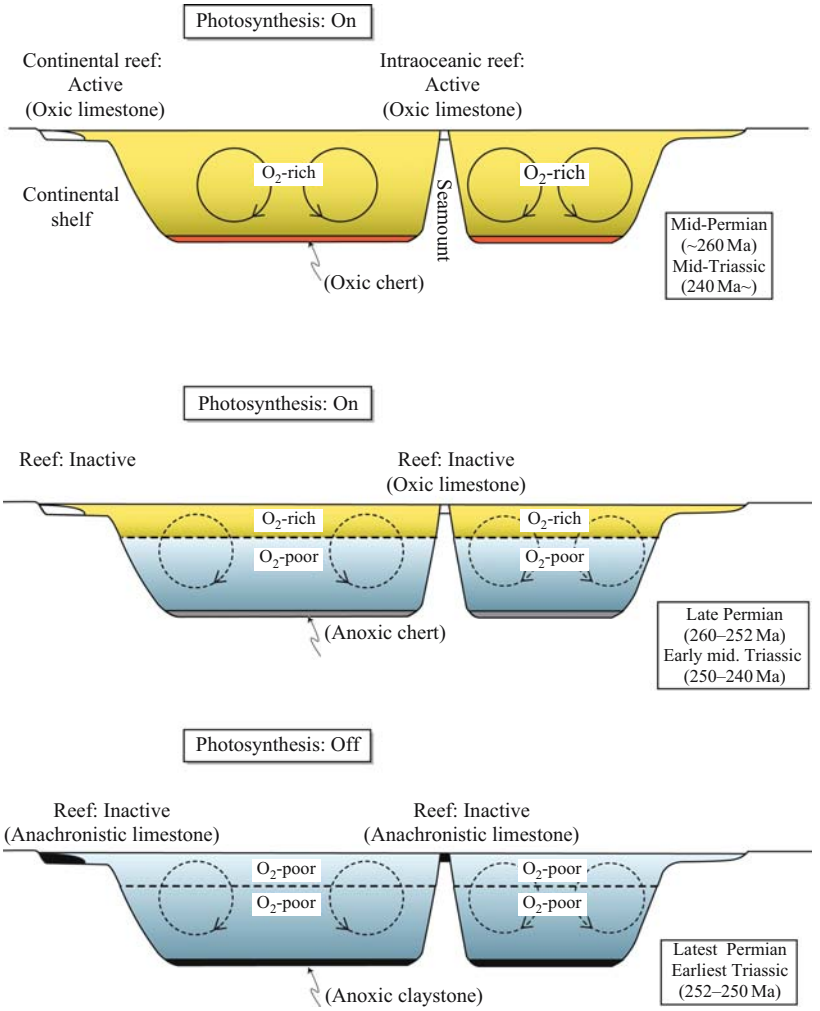


Figure 4. Schematic diagram of three modes of the superocean Panthalassa, showing the waxing and waning of the P-TB superanoxia (modified from Isozaki, 1996). The development of the superanoxia was monitored in three distinct lithofacies; continental shelf carbonates, mid-oceanic atoll carbonates, and deep-sea cherts. Top: Before the G-LB (ca. 260 Ma) and after the mid-Anisian (ca. 240 Ma), the whole superocean was healthy with oxygenated waters both in surface and bottom under effective oceanic circulation/mixing and resultant deep-sea ventilation. Middle: In the Late Permian (ca. 260–252 Ma) and most of the Early Triassic (ca. 250–240 Ma), deep superocean was anoxic while its shallow part remained oxygenated with active photosynthesis on surface. Bottom: Across the P-TB (ca. 252–250 Ma), the shallow superocean was also involved in the anoxia. In such an extreme condition, the global photosynthesis was likely shut down or considerably suppressed to drive the surface water anoxic regardless of oceanic circulation. This symmetric mode change during the 20 million year-long interval across the P-TB suggests that prolonged Earth-bound processes were responsible for the end-Paleozoic event rather than short-term episodic causes such as bolide impact and sudden methane release.

This supercontinent existed for nearly 100 million years until it broke apart in the Late Triassic by the opening of the new Atlantic Ocean. Concerning a possible connection of Pangea to the P-TB mass extinction and superanoxia, its breakup appears more important than its assembly.

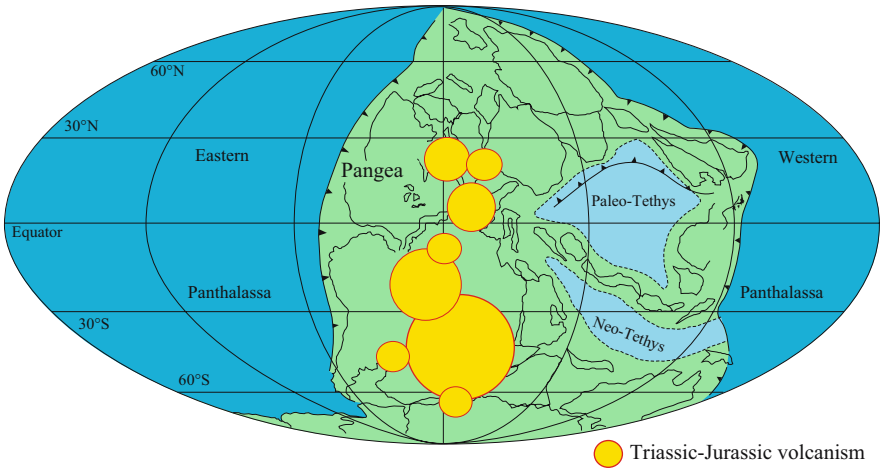
In general, continental breakup is regarded as a consequence of episodic activity of large mantle plumes (e.g., Maruyama, 1994; Ernst and Buchan, 2003). Particularly noteworthy is an extraordinarily large plume over 1000 km in diameter (a superplume) that represents the largest flow of material and of energy from the interior to the surface of the planet Earth. When the head of a superplume reaches the base of the overlying lithosphere, decompressional partial melting of mantle peridotite occurs in association with large-scale melting of pre-existing crustal rocks to generate extensive magmatism that results in formation of a large igneous province (LIP), one consequence of which is continental flood basalt (CFB) (or plateau basalt).

The main phase of Pangean breakup gave rise to the opening of the Atlantic Ocean in the Early Jurassic. A series of mantle plumes aligned in a N–S direction was responsible for the opening of this new ocean, and the remnants of the plumes are now observed as the voluminous volcanic rocks and dyke swarms in the Central Atlantic Magmatic Province (CAMP) along both sides of the Atlantic margins (Marzoli et al., 1999) (Fig. 5a). Prior to the opening of a new ocean, the breakup of a supercontinent was expressed by an initial rifting stage, in which the pre-existing continental crust is attenuated in an extensional tectonic regime induced by an uprising superplume. The development of the Late Triassic Newark rift basins coupled with the frequent intrusion of the Palisade Sills in the eastern USA represents direct consequences of such extensional tectonics associated with the continental breakup.

The above-mentioned volcanism and rift-related geological features are, however, obviously too young to be responsible for the P-TB extinction. The breakup of the supercontinent did not start from a single plume, because there are more plume remnants in the rest of Pangea that are much older. These include CFB of the Siberian Traps in Siberia, the Emeishan Traps in South China, the Panjal Traps in India, and alkaline volcanic rocks/intrusions in Oman, W. Australia, and Norway (Fig. 5b). Their contemporaneity with the proximal ages of the P-TB and G-LB extinctions have led many geologists to discuss possible causal links between the CFB volcanism and the mass extinction, and putative plume-generated large-scale volcanism is often regarded as the ultimate cause of the biggest mass extinction of the Phanerozoic (e.g., Renne and Basu, 1991; Campbell et al., 1992; Veevers and Tewari, 1995; Chung et al., 1998; Courtillot, 1999). In contrast, plate tectonic-driven (subduction- and ridge-related) magmatism occurred almost at a steady state throughout the entire Phanerozoic, thus had nothing to do with rare and unique geologic events that gave rise to major mass extinctions.

The secular change in initial $^{87}Sr/^{86}Sr$ isotope ratio of marine carbonates reflects that of contemporary seawater. The Phanerozoic $^{87}Sr/^{86}Sr$ curve (Fig. 6; Veizer, 2003; McArthur and Howarth, 2004) clearly demonstrates that the input of continental material into the oceans was suppressed most at the G-LB to give rise to the lowest initial $^{87}Sr/^{86}Sr$ ratio of the Paleozoic, probably implying the zenith (maximum assembly)

(a) Plume-related volcanism in the Triassic and Jurassic (200–170 Ma) (CAMP domain)



(b) Plume-related alkaline volcanism in the Late Permian (260–250 Ma)

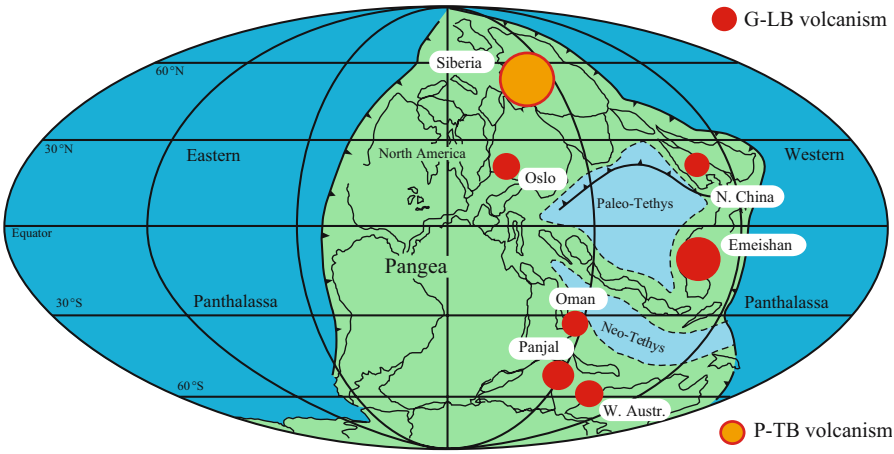


Figure 5. The mantle plume-derived large igneous provinces (LIPs) and relevant alkaline intrusions emplaced during the breakup of the supercontinent Pangea (base map from Scotese and Langford, 1995). a: The Triassic to Jurassic LIPs relevant to the opening of the Atlantic ocean (Central Atlantic Magmatic Province; CAMP; Maruyama, 1994); b: The Late Permian LIPs and major alkaline complexes including the continental flood basalts of Siberian (Russia), Emeishan (South China/Vietnam), and Panjal (India) Traps. The alkaline intrusive complexes, comprising syenite, nephelinite, lamproite etc., probably formed in relation with rifting under extensional tectonic regime. Two distinct phases of plume activity are recognized in the Pangea domain, one in the Late Permian and the other in the Triassic-Jurassic. It is noteworthy that the area of plume impingement shifted from the eastern half of Pangea in the Permian (b) to the western half in the Triassic-Jurassic (a). This apparent shift in activity center may have reflected heterogeneous conditions of the mantle beneath Pangea, or major morphological change of the superplume such as branching into several secondary plumes at the mantle transition zone ca. 400–660 km deep.

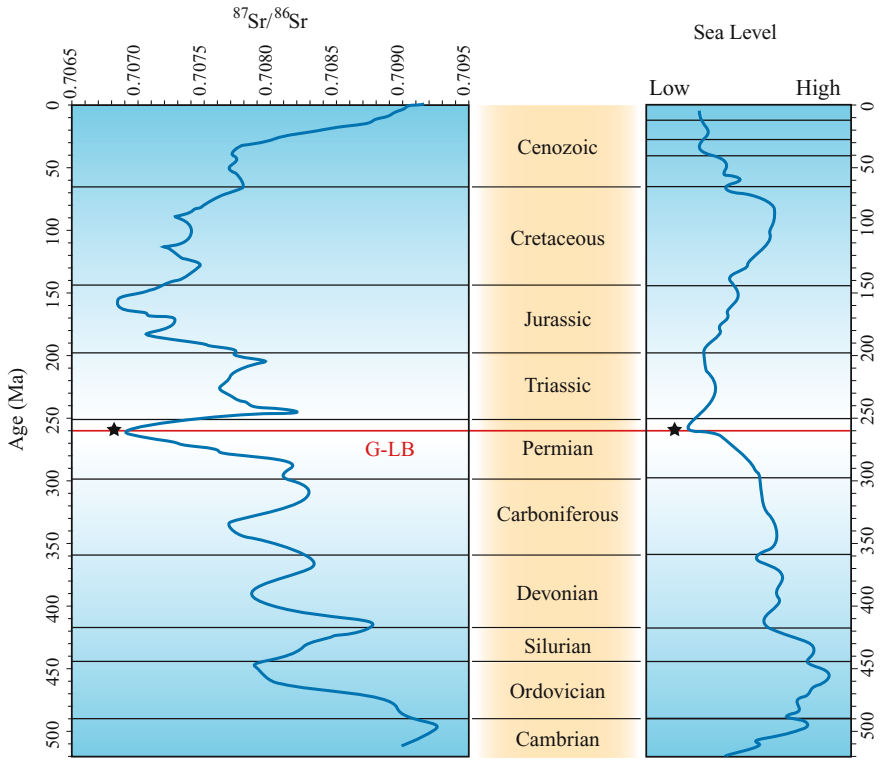


Figure 6. Phanerozoic secular change of initial $^{87}Sr/^{86}Sr$ isotope ratio of seawater (McArthur and Howarth, 2004) and relevant sea level change (modified from Hallam, 1992; Hallam and Wignall, 1999; Tong et al., 1999). Note that both the lowest value of $^{87}Sr/^{86}Sr$ ratio and the lowest sea-level of the Phanerozoic occurred not at the P-TB but around the G-LB. During the Pangean assembly in the Carboniferous to Middle Permian, continental drainage systems shrunk in total to decrease terrigenous supply to the superocean, thus to lower the seawater $^{87}Sr/^{86}Sr$ ratio. As triggered by the initial plume impingement beneath Pangea at the G-LB, the initial rifting in the eastern Pangea opened new drainage systems to put continental material with high $^{87}Sr/^{86}Sr$ ratio into the superocean. Plume-related excess input of volcanogenic CO_2 to atmosphere may have started global warming and sea-level rise toward the Mesozoic. The G-LB event rather than the P-TB event potentially marks the critical turning point from the Paleozoic to Mesozoic regime in various geological aspects.

of Pangea caused by the closure of pre-existing small oceans between continental blocks. In turn, in the Late Permian, the initial $^{87}Sr/^{86}Sr$ ratio started to increase rapidly, suggesting that the supply of weathered continental material to the oceans revived probably by continental rifting and the appearance of new intracontinental drainage systems. Thus the initial breakup of Pangea likely started not in the Early Triassic but already at the time of the G-LB in the Permian, considerably before the opening of the Atlantic in the Jurassic.

3 ENIGMA OF THE LATE PERMIAN VOLCANISM

Concerning a possible link between the large-scale volcanism and the P-TB and G-LB mass extinctions, most previous discussions have focused on the apparent chronological coincidence between the mass extinctions and CFB volcanism. This type of approach may suggest a possible causal link; however, it cannot establish its validity without other independent geological hard evidence, as in the case of the early K-TB controversy in which geochronological data alone were unable to determine whether volcanism or extraterrestrial impact was responsible for the extinction. Thus we must examine material-based geological evidence in various P-TB sections that can link volcanism to biospheric perturbation including extinction. The occurrence of tuff bed at the P-TB and G-LB horizons (Fig. 7) provides promising information for this approach, because they represent sole direct results of volcanism identified at the extinction horizons.

3.1 P-TB tuffs

The P-TB sections in South China contain remarkable evidence of volcanism adjacent to the mass extinction horizon in more than 35 sections including the GSSP at Meishan in Zhejian (e.g., Yin et al., 1993; Yang et al., 1991; Li et al., 1991). In the Meishan section, the top of Bed 24, marking the main extinction horizon, is directly overlain by an altered tuff (Bed 25, Fig. 7c). Also in the well-studied Shangsi section in Sichuan, several altered tuff beds occur around the P-TB (Li et al., 1989; Mundil et al., 2004). The P-TB tuffs have 1) euhedral phenocrysts, such as β-quartz, zircon and apatite, 2) pumice and/or glass shards, and sometimes show 3) porphyritic texture, suggesting that they were derived from explosive magma of felsic to intermediate composition (Yin et al., 1993). In the Chaotian section in Sichuan, 11 felsic tuff beds are concentrated within the 3 m-thick P-TB interval, suggesting a link between the violent volcanism and extinction-relevant environmental change (Isozaki et al., 2004, 2007b in press). Judging from the widespread occurrence of P-TB felsic tuff beds extending from Zhejian through Sichuan to Guangxi provinces (Figs. 7b–d), a remarkably large volcanic explosion likely caused the whole of South China to be covered with volcanic ash around the time of the P-TB, although the source volcano(s) has not yet been located. The so-called P-TB clay beds in Iran, Transcaucasia, and the Alps (Yin et al., 1993), and rhyo-dacitic tuff in Oman and Primorye in Russia (Rabu et al., 1990; Zakharov et al., 1995) should be re-examined in more detail.

3.2 G-LB tuff

A remarkable tuff bed characterizes the G-LB sections in South China. In contrast to the P-TB tuff beds, the G-LB tuff forms only one bed but is much thicker, 1–2 m (Fig. 7a). The G-LB tuff in South China was previously called the Wangpo bed (Lu, 1956; Li et al., 1991) and regarded as a terrigenous claystone until Isozaki and Ota

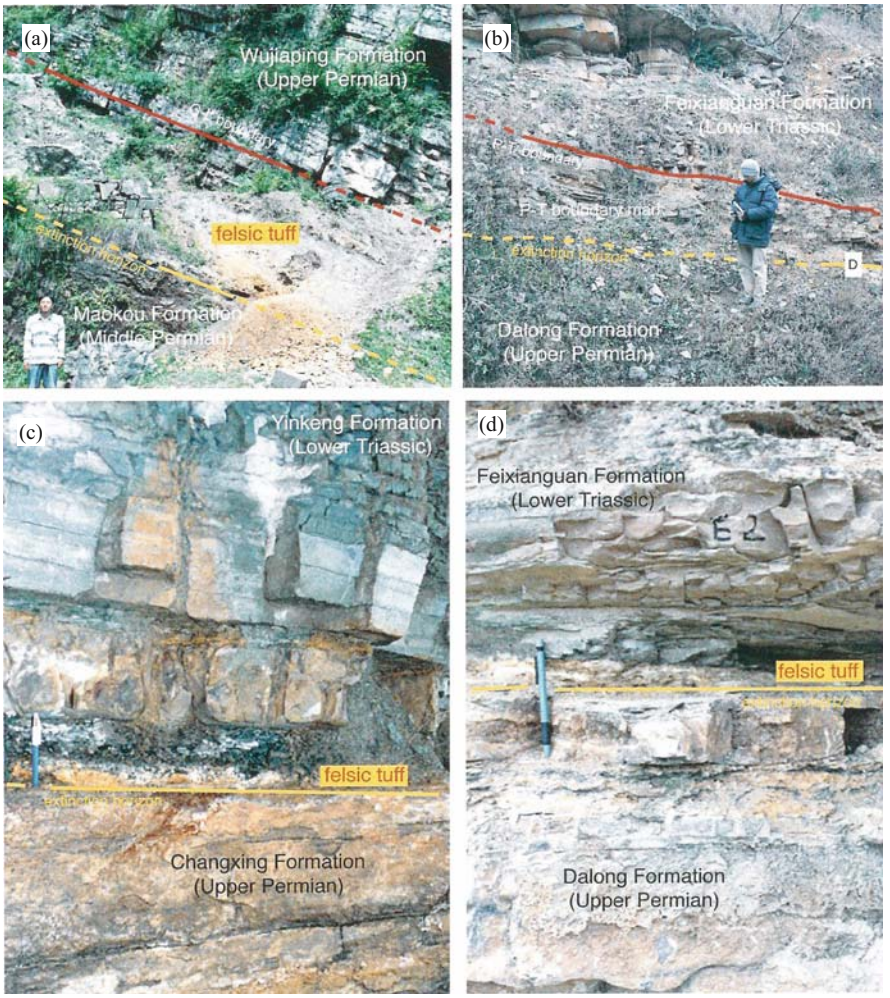


Figure 7. Field occurrence of the G-LB and P-TB felsic (rhyo-dacitic) tuffs in South China. a: G-LB tuff (2 meter thick; locally called the Wangpo bed) at Chaotian in northern Sichuan, b, d: P-TB tuff at Chaotian (Bed E1) (refer to Isozaki et al., 2004, 2007b in press), c: P-TB tuff (Bed 25) at Meishan in Zhejiang (refer to Yin et al., 1993, 2001). The abundant occurrence of zircon, β-quartz, and apatite phenocrysts suggests their origin from felsic alkaline magmatism rather than flood basalts (Siberian and Emeishan Traps). These boundary tuff beds occur mostly throughout South China, suggesting an extensive coverage of air-fall ash and a great magnitude and violent nature of source volcanisms.

(2001) pointed out its volcanogenic nature. This is an altered tuff (weathered into soft clay) that contains abundant euhedral phenocrysts such as β-quartz, plagioclase, zircon and apatite, suggesting that the source magma had a felsic to intermediate composition. According to this unique tuff within carbonate-dominant Permian sequence,

the Wangpo bed serves as a significant marker throughout South China, recognized in many sections (including its type locality in Lianshan, Shaanxi), in Chaotian, Shangsi, Emei-Ebian, Huaying (Sichuan), and Zhonghuopu (Hunan) (Li et al., 1991; Isozaki et al., 2004). It covers an area of nearly 1000 km N–S and 500 km E–W. Its regional extent within south China and its thickness of over 1 m require that the source volcano(s) was of enormous size, and that it was an explosive eruption with a felsic to intermediate composition.

Furthermore, Isozaki and Ota (2001) and Isozaki et al. (2004) pointed out the correlation between the mid-oceanic tuff beds and the Wangpo bed in South China. The occurrence of air-borne rhyo-dacitic tuff beds in mid-oceanic carbonate buildups further supports the large magnitude of the G-LB volcanism (Isozaki, 2007). As these rocks in Japan form exotic blocks secondarily incorporated in the Jurassic accretionary complexes, their primary sites of deposition were in the middle of the superocean Panthalassa off South China, probably over 3000 km to the east. The felsic volcanic ash was deposited in the mid-Panthalassa domain, at least in its western half, at the time of G-LB. In addition, the Upper Permian accretionary complex in Japan also contains G-LB rhyo-dacitic tuffs (tuff and tuffaceous mudstone; Nishimura et al., 1989); the felsic tuffs were deposited in a hemipelagic domain in western Panthalassa off Permian Japan (= South China) and were accreted to the Japan margin in the latest Permian. Their total thickness is over 100 m, though diluted by mud, that is much greater than that in the Jurassic complex, probably reflecting proximity to its source (Isozaki, 2007). Judging from such a difference in thickness, the relevant ash probably came from somewhere to the west of Panthalassa. It seems likely that western Panthalassa, together with South China, was extensively covered by air-borne ash of felsic composition at the G-LB. An extremely large, highly explosive felsic volcano(s) in western Pangea can explain both the long-distance delivery and huge volume of tuffaceous material in South China and western Panthalassa.

3.3 Volcanism at extinction boundaries: felsic vs. mafic

Based on their chronological coincidence, CFB are often regarded as the ultimate cause of the mass extinction (e.g., Courtillot, 1999; Ernst and Buchan, 2003; Wignall, 2001). For the P-TB and G-LB extinctions, the Siberian Traps and Emeishan/Panjal Traps (Fig. 5b) are nominated as the most popular candidates, respectively (e.g., Renne and Basu, 1991; Campbell et al., 1992; Chung et al., 1998).

Concerning the P-TB event, the Siberian Traps in Siberia (Fig. 5b) have the largest total volume and flow area of any CFB of ancient LIPs (e.g., Reichow et al., 2002; Saunders et al., 2005). By assuming the apparent coincidence in timing between the extinction and CFB, possible scenarios have been proposed to explain the volcanogenic catastrophe through aerosol-derived acid rain and/or volcanic gas-driven global warming (e.g., Campbell et al., 1992; Veevers and Tewali, 1995; Kozur, 1998; Racki and Wignall, 2005).

Although its initial eruption age has been controversial, it has recently been constrained to 251.7 ± 0.4 Ma by the latest U-Pb technique (Kamo et al., 2003). The age

of the P-TB extinction is dated as 252.4 ± 0.3 Ma at Meishan or 252.6 ± 0.2 Ma at Shangsi (Mundil et al., 2004). Comparing the ages of extinction and CFB volcanism, we admit that there is still an appreciable gap between the two events with respect to the error range, and that the extinction apparently predates the volcanism by 1–2 m.y.

For the cause of the G-LB extinction, the Emeishan Traps in western South China and the Panjal Traps in northern India (Fig. 5b) are likewise favored by many because of their apparent coincidence in timing (e.g., Chung et al., 1998; Zhou et al., 2002; Ali et al., 2002). Recent dating results of the Emeishan Traps identified the main eruption age at 256–259 Ma (Zhou et al., 2002), whereas age constraints for the Panjal Traps are not enough for precise correlation. The age of the G-LB mass extinction has not been tightly constrained yet but an age of 260.4 ± 0.7 Ma is proposed in the latest time scale (Gradstein et al., 2004). Like the P-TB case, the trap volcanism apparently postdates the mass extinction; it may thus not be the main cause. This age gap may become greater because the G-LB horizon is defined by the first appearance datum (FAD) of a new fossil taxon that belongs to the Lopingian (Upper Permian) fauna. The main extinction horizon of the Guadalupian (Middle Permian) fauna is located at a relatively low horizon below a post-extinction barren interval (e.g., Ota and Isozaki, 2006).

In all previous discussions on possible cause–effect relationships, the absence of material-based hard evidence that directly links the two independent events, i.e., extinction and CFB volcanism, remains a major obstacle regardless of the credibility of coincidence in mutual timing. In addition, the basaltic geochemistry of these CFB examples can explain neither the violent explosive eruption nor the felsic nature of the P-TB and G-LB tuffs. In fact, some andesitic basalt and rhyolite units occur in the CFBs, but they are confined not to the basal parts of the traps but to the middle-upper part (e.g., Xu et al., 2001) and they are too small in volume to account for the entire coverage of the above-mentioned regional tephra. Thus andesitic basalt and rhyolite units within the traps are not the likely source of the felsic tuffs at both the P-T and G-L extinction boundaries. The boundary tuffs in South China and Panthalassa represent the only available hard evidence that can link volcanism with the two major mass extinctions; therefore, their unique felsic nature needs a more detailed scrutiny.

4 ALKALI MAGMATISM

To seek a possible link between large-scale felsic volcanism and Pangean breakup, unique alkaline magmatism is the focus of this section. The breakup of a supercontinent is likely related to mantle plume activity (e.g., Maruyama, 1994; Ernst and Buchan, 2003) that often leaves relevant LIPs associated with extensional tectonic features. LIPs in mid-continental rifts or rifted continental margins are mainly composed of CFB that are often associated with alkaline igneous rocks.

Modern and ancient alkaline igneous suites in large, ring-shaped intrusive complexes show a great variety of rock types; e.g., nepheline syenite, phonolite, nephelinite, ijolite, and lamproite. Such a wide diversity in alkaline rocks, from ultramafic to felsic composition, is generally explained in terms of magmatic interaction between mantle-derived primordial magma and pre-existing, already differentiated lithospheric rocks (e.g., Sorensen, 1974; Bell, 1989).

As mentioned above, the putative G-LB and P-TB felsic volcanisms were unusually large-scale and quite distinct from plate tectonic-driven volcanism along island arcs and mid-oceanic ridges. Volcanism in arcs and ridges continuously maintains its activity as long as plate tectonics is in operation, thus such continuous volcanism probably has nothing to do with rare and catastrophic events like major mass extinctions that occurred only five times in the ca. 550 million year-long Phanerozoic. The other possible felsic magma source exists solely at a hotspot, in particular that located on the continental lithosphere, where a mantle plume differentiates magma into various compositions. Therefore, the episodic felsic volcanism at the G-LB and P-TB were likely related to alkaline volcanism induced by non-steady-state or non-plate-tectonic magmatism associated with a mantle plume.

In this regard, the common occurrence of apatite phenocrysts both in the G-LB and P-TB tuffs (Isozaki et al., 2004, 2007b in press; Yin et al., 1993) is noteworthy because apatite commonly occurs in alkaline rocks reflecting the enrichment of phosphorous in alkaline magma. This positively suggests that felsic to intermediate magmatism of the alkaline rock series was involved in the two boundary events.

In South China, major Permian intrusive complexes are composed of syenite, essexite, and alkali gabbro. For example, the kilometer-size Baima, Maomaogou and Panzhihua intrusive complexes in southern Sichuan are composed of nepheline syenite, including some up to 10 km $\times$ 20 km (Co-operative Geological Research Group of Japan and China in the Panxi Region, 1986), and were dated as 252–255 Ma (Lo et al., 2002). They may represent the source of the latest Permian felsic tuffs, although their effusive counterparts have not so far been recognized, probably owing to surface erosion. The occurrence of such large-scale alkaline complexes in the vicinity of the Emeishan CFB in South China suggests that at least one plume head (not necessarily a superplume but probably a smaller branched secondary plume) has impinged beneath South China in the Late Permian.

The occurrence of thick felsic tuffs in uppermost Permian shelf sediments in Primorye (Zakharov et al., 1995) suggests that similar violent volcanism affected Far East Russia around the P-TB timing. The ring-shaped Maimecha-Kotui alkaline-ultramafic complex (253 Ma) in Siberia is likely a remnant of such alkaline magmatism induced by a mantle plume (Basiliev and Zolotukhin, 1995); however, no effusive counterparts of felsic to intermediate composition are known. More work is needed from high-resolution volcanic stratigraphy coupled with geochronology in regions with contemporary CFBs, such as South China, Siberia, and northern India. Also in the rest of the world, similar alkaline intrusive complexes of similar age to the P-TB and G-LB should be checked in this regard. Possible candidates of such Permian alkaline intrusives include those in southern Norway, Oman, and W. Australia

(Neumann et al., 1992; Rabu et al., 1990; Le Maitre, 1975; Veevers and Tewari, 1995; Fig. 5b).

Among these alkaline rocks, although not so large in extent, some have highly distinctive composition, such as carbonatite and kimberlite. Carbonatite commonly occurs in close association with the above-mentioned alkaline silicate rocks in large intrusive bodies (Bell, 2001). Recently the occurrence of Permo-Triassic carbonatites was reported in North China, Tarim, and the North/South China border (Yang and Woolley, 2006). Kimberlite is another diagnostic rock in the alkaline suite. Besides its diamondiferous nature, kimberlite has a unique mode of occurrence as a diatreme or a pipe that is generally regarded to have formed through a highly explosive eruption, in accordance with the high content of its volatile components (Mitchell, 1991). Alkaline volcanism, sometimes accompanying kimberlite and carbonatite in the early stage, may drive violent eruptions (Bell, 2001) because the relevant magmas can carry huge amounts of a gas phase. Carbonatites occur preponderantly in North China and Tarim, probably reflecting the development of an Archean tectosphere (continental keel) enriched in carbon.

Isozaki (2000, 2001) speculated that such a highly explosive eruption by rapidly ascending kimberlite from the deep mantle rather than CFB *per se*, may have caused the remarkable biospheric perturbation at the P-TB. From a theoretical viewpoint, Morgan et al. (2004) recently proposed a similar interpretation (Verneshot hypothesis) to explain a possible general link between plume activity and mass extinction. Alkaline magmatism, in particular from a kimberlitic eruption, may represent a precursor of plume-related magmatism prior to the main eruption of CFB as suggested from the mode of occurrence of kimberlite with respect to CFB (e.g., kimberlite pipe fields were buried under CFB in Deccan and Siberia) and from pressure-temperature conditions in the subcontinental mantle capable of generating a carbon-rich magma (e.g., Morgan et al., 2004).

I emphasize here that both the G-LB and P-TB biospheric turnovers were probably triggered not by CFBs but by violent alkaline magmatism possibly including kimberlite/carbonatite intrusions, and that all this volcanism was essentially driven by the impingement of a superplume beneath the supercontinent Pangea. To date, however, such a link between kimberlite eruption and mass extinction has not yet been proven in any mass extinction event of the Phanerozoic on the basis of substantiated evidence. Neither kimberlite nor carbonatite can form felsic tuffs at the extinction boundary horizons, probably because they usually do not leave large amounts of lava/pyroclastics and tuffs. In this respect, kimberlite/carbonatite eruption alone cannot explain the extensive delivery of felsic ash at the boundaries, and the nature of the contemporary alkaline volcanism should be further clarified.

5 PLUME WINTER: A POSSIBLE SCENARIO

In order to explain the felsic tuffs closely associated with the G-LB and P-TB mass extinction horizons, the possible scenario of a “Plume Winter” was proposed by Isozaki (2000, 2001). This may sound similar to the recent popular idea of

linking CFB and mass extinction at both the G-LB and P-TB (e.g., Courtillot, 1999; Wignall, 2001; Racki and Wignall, 2005). However in the "Plume Winter" hypothesis, the emphasis is placed not on CFB basalt but on alkaline magmatism (including carbonatite/kimberlite) and its effect on the biosphere.

The scenario is simple and straightforward, if we assume plume-induced violent volcanism was the cause of the biospheric perturbation (Figs. 8, 9). When a plume head impinged at the lithosphere/asthenosphere boundary beneath the supercontinent Pangea, mantle-derived primordial magmas induced melting/metasomatism of pre-existing continental lithosphere to generate diverse magmas with alkaline signatures. Partial melting in shallow crustal levels gave rise to highly explosive alkaline volcanism of felsic to intermediate composition prior to the eruption of voluminous CFB. The alkaline lavas may have been associated with kimberlite/carbonatite, highly enriched in volatile components, such as CO_2 and SO_2, particularly in the early stage. As they were transported rapidly to the surface, they generated extraordinary large explosive eruptions. In domains above plumes, swarms of kimberlite/carbonatite may have become activated to leave a profound impact on the surface environment, although each intrusion or diatreme/pipe was small.

Such violent volcanism might directly cause 1) delivery of air-borne ash of felsic-intermediate nature over extensive areas, 2) formation of a dust/aerosol-screen in the stratosphere, and 3) input of CO_2 and SO_2 to the atmosphere. These phenomena would be followed by 4) decrease in insolation on the Earth's surface, 5) lowering of the surface temperature, and 6) pouring of acid rain; these were all critical for maintaining a pre-existing food web system in the biosphere. In particular, the combination of dim light, coldness, and highly acidic surface water may have severely destroyed the photosynthesis-driven primary productivity on both land and sea that formed the base of the food web on a global scale. A sharp decline or even temporary cessation of the primary production may have triggered cascaded extinctions of marine and terrestrial heterotrophic animals, firstly herbivorous, then carnivorous. Possible kill mechanisms include also volcanogenic heavy metal poisoning and volcanic gas-induced troubles in respiratory/circulatory or nerve systems in biota, in particular for those dependent on O_2 respiration. The deep-sea oxygen depletion may have been triggered by a temporary crash of photosynthesis rather than sluggish oceanic circulation as suggested by many (e.g., Hotinski et al., 2001). The following alkaline magmatism of the main phase delivered a large quantity of air-borne felsic ash, and CFB in the later stage added huge amount of CO_2 to turn the environment into a global warming trend that not merely enhanced the deep-sea anoxia by slow oceanic circulation but also delayed the biotic recovery.

The greatness of the end-Permian biospheric crisis is regarded as the combined consequence of two independent events, one at the G-LB (ca. 260 Ma) and the other at the P-TB (ca. 252 Ma), that occurred in a relatively short time interval of less than 10 million years (Stanley and Yang, 1994). The two end-Paleozoic mass extinctions likely occurred in two episodes of "Plume Winter" related to two independent activity-highs of mantle plume (Fig. 10). Nearly 8–10 million years after the initial development of deep-sea anoxia, by invading shallow marine environments on the

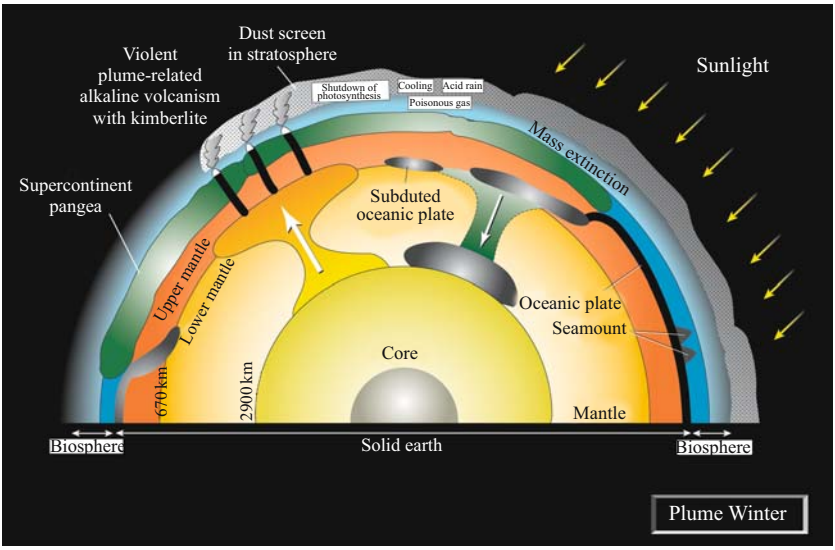


Figure 8. Schematic diagram of the "Plume Winter" scenario. The ascent of a superplume beneath the supercontinent Pangea was the most likely ultimate cause of the double-phased mass extinction at the G-LB and P-TB, as a mantle superplume represents the largest flow of material and of energy within the planet Earth. Up-rising hot plumes paired with a down-going cold plume form a large-scale whole-mantle convection cell; however, their behavior is not smooth/continuous but intermittent as paced in the mantle transition zone (ca. 400–660 km deep). Break-up of a supercontinent is intimately linked to the impingement of a superplume-head at the base of a supercontinental lithosphere. Prior to the final breakup of a supercontinent coupled with opening a new ocean, the initial stage of rifting is characterized by precursory alkaline magmatism that includes kimberlite/carbonatite enriched in volatile components. High temperature alkaline magma generated in the upper mantle re-melts pre-existing lower crust of a supercontinent to generate felsic to intermediate, alkaline magmatism before the outpouring of continental flood basalt (CFB) in a later stage of rifting. An extraordinarily explosive volcanism in the earlier stage of such plume-induced magmatism may cause various unusual impacts on the surface environments, in particular on the biosphere. Direct volcanogenic deterioration includes formation of a dust/aerosol screen in the stratosphere, gas poisoning, lowering of surface temperature, and acid rain. Among everything else, the shutdown of sunlight and global cooling by the dust/aerosol screen appear the most significant because the cessation of photosynthesis on a global scale is critical in maintaining bio-productivity. A short-time darkness and coldness can halt photosynthesis on a global scale and disorganize the pre-existing food web. Increase of atmospheric CO_2 by alkaline magmatism and later CFB causes global warming to drive prolonged anoxia and the delayed recovery of biodiversity. In the case of the Paleozoic-Mesozoic transition, the African superplume, probably its secondary branched plumes, ascended beneath Pangea in two phases, i.e., at the G-LB and P-TB, driving two episodes of "Plume Winter".

peri-Pangean continental shelves with oxygen-depleted water, the superanoxia likely culminated at the time of P-TB when the second "Plume Winter" (Plume Winter II) occurred.

From a long-term viewpoint, the G-LB event (Plume Winter I) appears more important than that at the P-TB (Plume Winter II) (Fig. 10) because all the global geological

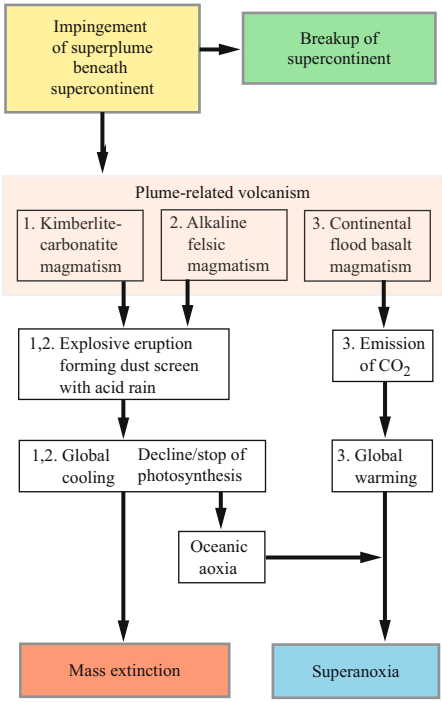


Figure 9. Flow chart of the end-Paleozoic "Plume Winter" scenario. The impingement of the African superplume head beneath the supercontinent Pangea caused the three unique geological phenomena at the Paleozoic/Mesozoic transition, viz. the initial breakup of Pangea, the development of superanoxia, and the greatest mass extinction of the Phanerozoic (Fig. 1). The key process that linked these global geological phenomena unique to the P-TB was extraordinarily violent volcanism induced by the superplume. Plume-related magmatism was three-fold; i.e., 1) precursory kimberlite/carbonatite, 2) alkaline felsic-intermediate volcanism, and 3) continental flood basalt. The former two were responsible for the mass killing through explosive eruptions forming dust/aerosol screen, while the latter for the prolonged anoxia and delayed recovery through global warming.

phenomena, including the superanoxia and decline in biodiversity, started at the time of G-LB as emphasized by Isozaki (1997). It is also noteworthy that the plume activity related to the Pangean breakup became apparent for the first time not in the Triassic-Jurassic time but already in the late Middle Permian. The following independent lines of evidence support this view. The secular changes in the global sea-level curve (Hallam and Wignall, 1999; Tong et al., 1999) and in the initial $^{87}Sr/^{86}Sr$ isotope ratio (Veizer, 2003; McArthur and Howarth, 2004) clearly show a sharp turning point around the G-LB (Fig. 6). Both signatures are regarded as reflecting the beginning of a new plume activity at the Earth's surface at the time of the G-LB. Global sea level hit its lowest level in the Phanerozoic around the G-LB, and then started to rise almost uni-directionally in the Late Permian and Mesozoic (Hallam and Wignall,

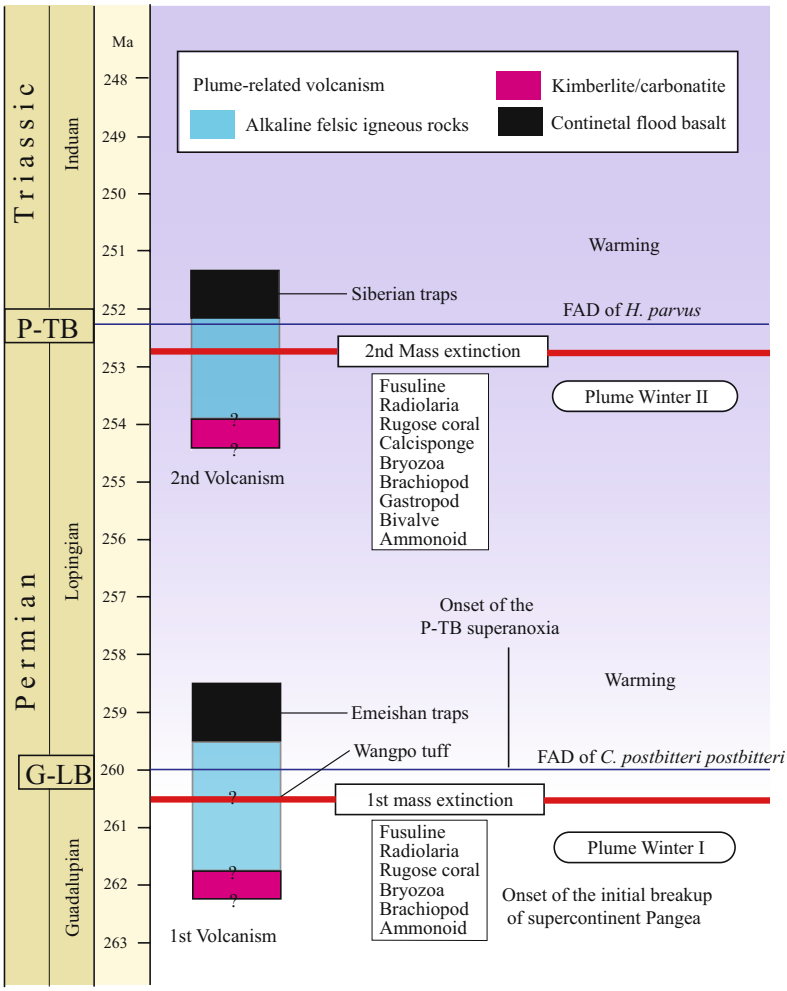


Figure 10. Schematic timetable of the end-Paleozoic global events with two episodes of "Plume Winter". The double-phased mass extinction corresponds to the double-phased plume-generated explosive volcanism of alkaline nature. Each event was large enough to change the surface environment and to terminate various animals on land and in sea; nonetheless, the greatest magnitude of the terminal Paleozoic extinction was achieved by two "Plume Winter" episodes occurring within a relatively short time interval (less than 10 million years) that did not allow full biotic recovery after the first event. Note that the mass extinction predated the CFB volcanism in both the G-LB and P-TB cases.

1999). A short-term cool period was newly detected by stable carbon isotope analysis of marine carbonates in uppermost Middle Permian atoll limestone in the low latitude domain of Panthalassa (Isozaki et al., 2007a) in accordance with the low sea-level, and this appears to have been coeval with the claimed "Plume Winter I".

On the other hand, the initial $^{87}Sr/^{86}Sr$ ratio also hit a low in the uppermost Middle Permian and started to rise rapidly and uni-directionally in the Late Permian and Triassic (Fig. 6; e.g., Veizer, 2003; McArthur & Howarth, 2004; Fukui et al., 2005). Low $^{87}Sr/^{86}Sr$ values of seawater usually suggest a high stand of sea-level due to lesser erosion on continents and resultant lesser flux of continental crust-derived material enriched with radiogenic ^{87}Sr into oceans. In this context, the low $^{87}Sr/^{86}Sr$ values and low sea-level detected around the G-LB apparently contradict each other. However, this probably reflects the unique paleogeography at the initial breakup of the supercontinent around the G-LB that has controlled the drainage systems on Pangea. During most of the Early-Middle Permian when major continental blocks merged, nearly a half of the pre-existing river systems became highly restricted within Pangea, losing direct passage to the superocean, and this resulted in lowering the seawater $^{87}Sr/^{86}Sr$ ratio to the Paleozoic minimum (Fig. 6). In turn, the plume-driven initial rifting of Pangea around the G-LB gave rise to rift-related new drainage systems connected to the superocean for the first time since the mid-Carboniferous, and this forced the $^{87}Sr/^{86}Sr$ ratio of the global seawater to start increasing.

Moreover, it is also worth noting that the magnetostratigraphic records demonstrate a clear mode change around the basal Capitanian (ca. 265 Ma; Late Guadalupian) immediately before the G-LB, from the long-term Kiaman Reverse superchron (throughout the Late Carboniferous and Early-Middle Permian) to the Permian-Triassic Mixed superchron with frequent polarity change (in the Late Permian and Early Triassic) (Fig. 11; Haag and Heller, 1991; Heller et al., 1995; Jin et al., 1997; Gradstein et al., 2004). This remarkable change called the Illawarra Reversal (Menning, 2000) probably reflects the appearance of thermal instability at the 2900 km-deep mantle/core boundary after a 60-m.y. long stable period, probably by the landing of a cold megalith (= cold plume or chunk of subducted slabs) onto the mantle/core boundary (Fig. 8). This may have affected the state of geodynamo by heat transfer from the core and initiated a superplume. The time lag between the Illawarra Reversal and the G-LB event is ca. 5 million years or less according to the timescale of Gradstein et al. (2004), and this may represent the travel time of a plume head from the lower mantle to the upper mantle above the 660 km-deep discontinuity. Judging from an estimated ascending rate of a mantle plume (several 10 cm/year), this time lag appears reasonable on the order of magnitude (M. Ogawa, personal communication). In contrast, the secondary plumes that affected the biosphere twice (at the G-LB and P-TB) were originated from the mantle transition zone (ca. 400–660 km deep) and did not cause any significant change on the core/mantle boundary and of the geodynamo in the outer core (Fig. 11).

This "Plume Winter" scenario (Figs. 8, 9) can thus reasonably explain not only the three major geological phenomena 1) the greatest mass extinction, 2) superanoxia, and 3) breakup of a supercontinent that occurred uniquely at the Paleozoic-Mesozoic transition (Fig. 1) but also the long-term changes in sea level, seawater $^{87}Sr/^{86}Sr$ ratio, and geomagnetic field behavior (Figs. 6, 11).

After the second episode (Plume Winter II), the accumulated atmospheric CO_2 and additional methane from clathrates may explain the global warming and sea-level

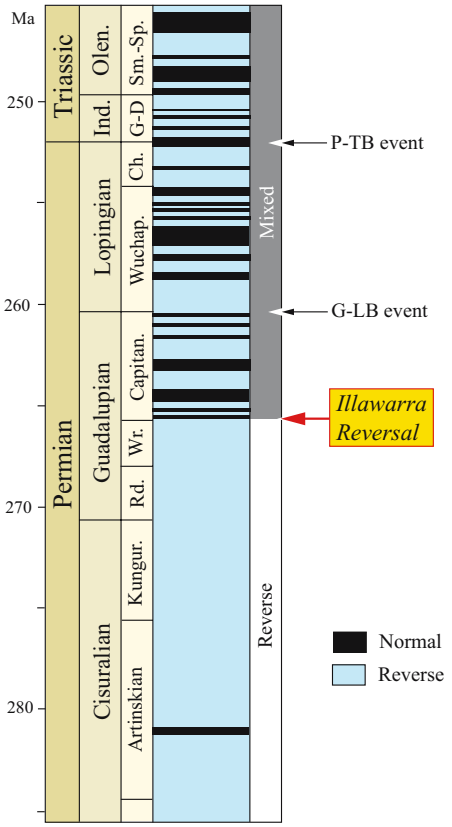


Figure 11. Geomagnetic field behavior in the Permian to Early Triassic and its possible link to the mass extinction events at the P-TB and G-LB (modified from Gradstein et al., 2004). A major change in geomagnetic filed behavior (Illawarra Reversal) occurred in the early Capitanian (Late Guadalupian) immediately before the G-LB event, from the long-term Kiaman Reverse superchron to the Permian-Triassic Mixed superchron with frequent fluctuation. This represents the most prominent marker in magnetostratigraphic correlation of the Late Paleozoic, suggesting that a cold megalith landed on the mantle/core boundary and a superplume was launched from the lower mantle in association with instability at the mantle/core boundary, changing the mode of geodynamo. The time lag between the Illawarra Reversal and the G-LB extinction event (ca. 5 million years or less) may represent a travel time of a superplume from the lower to upper mantle.

rise in the Early Triassic (e.g., Retallack, 1999; Hallam and Wignall, 1999). The global warming by excess greenhouse CO_2 may have accelerated the environmental deterioration and drove the prolonged deep-sea anoxia (Isozaki, 1994) and delayed recovery of biospheric structure until the Middle Triassic (Bottjer, 2004; Stanley, 1988), however, all these occurred in the Early Triassic nearly 10 million years after the first event at the time of the G-LB, just representing the aftermath of the double-phased “Plume Winter” episode.

6 CONCLUSIONS

The breakup of the supercontinent Pangea gave rise to the opening of the Atlantic and Indian oceans. Plural plumes became activated successively in the latest Paleozoic to Early Mesozoic, and rifted apart the pre-existing continental lithosphere to accommodate space for the new oceans, and the rifted continental margins of which are marked by LIPs and radial dike swarms. All these plumes activated beneath Pangea, including those at G-LB and P-TB, probably represent secondary plumes that branched off from a superplume in the mantle transition zone (Maruyama, 1994). Judging from the analyses of modern-day topography of Africa and of global seismic tomography (e.g., Fukao et al., 1994; Zhao, 2007 this volume), the main superplume responsible for the breakup of Pangea was located beneath Africa. Thus the G-LB and P-TB plumes mark the first impingement of the African superplume beneath the Pangean continental lithosphere. In addition to the widely known LIPs of Siberia, Emeishan and Panjal, more remnants of coeval branched plumes may be detected. It is noteworthy that the Late Permian LIPs were concentrated in the eastern half of Pangea, whereas the Triassic-Jurassic ones of CAMP domain in the western half (Fig. 5). This apparent shift of activity-center during a 100 million year interval may reflect a secular change in the behavior of the African superplume with respect to mantle heterogeneity or to change in plume geometry in the mantle transition zone.

This is in sharp contrast with the much older Pacific opening that occurred at nearly 700–750 Ma when the supercontinent Rodinia broke up (e.g., Hoffman, 1991; Dalziel, 1995). Remnants of this superplume can be recognized not only in the LIPs on former rifted continental margins but also in the modern southern Pacific, i.e., the Pacific superswell, over 2000 km in diameter, featuring plural hotspots (McNutt and Judge, 1990).

Thus with a long-term viewpoint, a major reorganization in mantle regime corresponds to the Wilson cycle in crustal plate tectonics. The Phanerozoic mantle regime is divided into two periods; earlier one controlled by the Pacific superplume and the later one by the African superplume, and these two correspond to the expanding period of the Pacific Ocean (late Neoproterozoic to Paleozoic) and that of the Atlantic–Indian ocean (Mesozoic to the present), respectively. In this context, the P-TB, previously recognized solely as a time of major reorganization of biota from the Paleozoic to the Mesozoic-Modern regime, in fact corresponds to the time of major re-organization of the mantle regime.

As summarized above, the end-Paleozoic mass extinction, i.e., the largest biospheric turnover in the Phanerozoic, occurred in the middle of global re-organization of the planet's interior. In the Precambrian, there should have been several major extinction events driven by similar causes; however, the rare occurrence of fossils, microbial remains in particular, has hampered detailed documentation of such unidentified cryptic extinction events. Nonetheless our curiosity is stimulated by the apparent coincidence in timing between the Neoproterozoic snowball Earth event (Kirschvink, 1992; Hoffman and Schrag, 2002) and the breakup of the supercontinent Rodinia (Hoffman, 1991), or that between the Paleoproterozoic snowball Earth

(Kirschvink et al., 2000) and the breakup of Neoarchean (super-)continent including Kenoria (Arctica) and/or Ur (e.g., Rogers and Santosh, 2004). A precise understanding of the Phanerozoic mass extinction events, in particular their cause–effect, will open a new window to look into the mysterious Precambrian biosphere and its evolution.

ACKNOWLEDGEMENTS

The author greatly appreciates constructive discussions with Shigenori Maruyama (Tokyo Inst. Tech.), Masaki Ogawa (Univ. Tokyo), language check by Brian Windley (Leicester Univ.), and help in drafting figures by Shio Watanabe.

REFERENCES

Ali, J.R., G.M. Thompson, X.Y. Song, and Y.L. Wang (2002) Emeishan basalts (SW China) and the 'end-Guadalupian' crisis: Magnetobiostratigraphic constraints. *J. Geol. Soc., London*, 159, 21–29.

Alvarez, W. (1997) *T. rex* and the Crater of Doom, Princeton Univ. Press, Princeton.

Basiliev, Y.R., and V.V. Zolotukhin (1995) The Maimecha-Kotui alkaline-ultramafic province of the northern Siberian platform, Russia. *Episodes*, 18, 155–164.

Basu, A.R., R.J. Poreda, P.R. Renne, F. Teichmann, Y.R. Vasiliev, N.V. Sobolev, and B.D. Turrin (1995) High-^{3}He plume origin and temporal-spatial evolution of the Siberian flood basalts. *Science*, 269, 822–825.

Baud, A., M. Magaritz, and W.T. Holser (1989) Permian-Triassic of the Tethys: Carbon isotope studies. *Geol. Rundschau*, 78, 649–677.

Becker, L., R.J. Poreda, A.R. Basu, K.O. Pope, T.M. Harrison, C. Nicholson, and R. Iasky (2004) Bedout: A possible end-Permian impact crater offshore of northwestern Australia. *Science*, 304, 1469–1474.

Becker, L., R.J. Poreda, A.G. Hunt, T.E. Bunch, and M. Rampino (2001) Impact event at the Permian-Triassic boundary: Evidence from extraterrestrial noble gases in fulleranes. *Science*, 291, 1530–1533.

Bell, K. (1989) Carbonatites: Genesis and Evolution, Unwin Hyman, London.

Bell, K. (2001) Carbonatites: Relationships to mantle-plume activity. In Ernst, R.E., and K.L. Buchan (eds.) Mantle Plumes: Their Identification Through Time, *Geol. Soc. Am. Special Paper*, 352, pp. 267–290.

Benton, M.J. (1985) Mass extinction of non-marine tetrapods. *Nature*, 316, 811–814.

Bottjer, D. (2004) The beginning of the Mesozoic: 70 million years of environmental stress and extinction. In Taylor, P.D. (ed.) Extinctions in the History of Life, Cambridge Univ. Press, Cambridge, pp. 99–118.

Campbell, I., G.K. Czamanske, V.A. Fedorenko, R.I. Hill, and V. Stepanov (1992) Synchronism of the Siberian traps and the Permian-Triassic boundary. *Science*, 258, 1760–1763.

Chung, S.L., B.M. Jahn, G.Y. Wu, C.H. Lo, and B.L. Cong (1998) The Emeishan flood basalt in SW China: A mantle plume initiation model and its connection with continental breakup and mass extinction at the Permian-Triassic boundary. *Am. Geophys. Union Geodynamic Ser.*, 27, 47–58.

Cirilli, S., C.P. Radrizzani, M. Ponton, and S. Radrizzani (1998) Stratigraphical and palaeoenvironmental analysis of the Permian-Triassic transition in the Badia Valley (Southern Alps, Italy). *Paleogeogr. Paleoclimat. Paleoecol.*, 138, 85–113.

Clark, D.L., C.Y. Wang, C.J. Orth, and J.S. Gilmore (1986) Conodont survival and low iridium abundances across the Permian-Triassic boundary in South China. *Science*, 233, 984–986.

Co-operative Geological Research Group of Japan and China in the Panxi Region (1986) Geology of the Panxi region, Sichuan province, southwest China, Yamaguchi Univ., Yamaguchi, 340p.

Courtillot, V.E. (1999) Evolutionary Catastrophe. The Science of Mass Extinction, Cambridge Univ. Press, Cambridge, 173p.

Dalziel, I. (1995) Earth before Pangea. *Scientific American*, 1995-1, 38–43.

Ernst, R.E., and K.L. Buchan (2003) Recognizing mantle plume and the geological record. *Ann. Rev. Earth Planet. Sci.*, 31, 469–523.

Erwin, D.H. (1993) The Great Paleozoic Crisis: Life and Death in the Permian. Columbia Univ. Press, New York, 327p.

Erwin, D.H., S.A. Bowring, and Y.G. Jin (2002) End-Permian mass extinctions: A review. *Geol. Soc. Amer. Spec. Pap.*, 356, 363–383.

Farley, K.A., P. Ward, G. Garrison, and S. Mukhopadhyay (2005) Absence of extraterrestrial ^{3}He in Permian-Triassic age sedimentary rocks. *Earth Planet. Sci. Lett.*, 240, 265–275.

Fukao, Y., S. Maruyama, M. Obayashi, and H. Inoue (1994) Geologic implication of the whole mantle P-wave tomography. *J. Geol. Soc. Jpn.*, 100, 4–23.

Fukui, M., T. Kani, H. Nohda, and Y. Isozaki (2005) Pb-Pb isochron age and Sr isotope study for the Middle-Upper Permian limestone in the Kamura area in Kyushu, Japan. Abst. Amer. Geophys. Union, V41F-1526.

Gradstein, F., J. Ogg, and A. Smith (2004) Geologic Timescale, Cambridge Univ. Press, Cambridge, 589p.

Grice, K., C. Cao, G.D. Love, M.E. Böttcher, R.J. Twitchett, E. Grosjean, R.E. Summons, S.C. Turgeon, W. Dunning, and Y.G. Jin (2005) Photic zone euxinia during the Permian-Triassic superanoxic event. *Science*, 307, 706–709.

Haag, M., and F. Heller (1991) Late Permian to Early Triassic magnetostratigraphy. *Earth Planet. Sci. Lett.*, 107, 42–54.

Hallam, A. (1992) Phanerozoic Sea-level Changes, Columbia Univ. Press, New York, 266p.

Hallam, A., and R. Wignall (1997) Mass Extinctions and their Aftermath, Oxford Univ. Press, Oxford, 320p.

Hallam, A., and P. Wignall (1999) Mass extinctions and sea-level changes. *Earth-Sci. Review*, 48, 217–250.

Heller, F., H.H. Chen, J. Dobson, and M. Haag (1995) Permian-Triassic magnetostratigraphy—new results from South China. *Phys. Earth Planet Inter.*, 89, 281–295.

Hoffman, P.F. (1991) Did the breakout of Laurentia turn Gondwanaland inside-out? *Science*, 252, 1409–1412.

Hoffman, P.F., and D.P. Schrag (2002) The snowball Earth hypothesis: Testing the limits of global change. *Terra Nova*, 14, 129–155.

Holser, W.T., H.P. Schönlaub, M. Attrep Jr., and 12 others (1989) A unique geochemical record at the Permian/Triassic boundary. *Nature*, 337 39–44.

Holser, W.T., and H.P. Schönlaub (eds.) (1991) The Permian-Triassic boundary in the Carnic Alps of Austria (Gartnerkofel region). *Abhandl. Geol. Bundesanst.*, 45, 1–232.

Hotinski, R.M., K.L. Bice, L.R. Kump, R.G. Najjar, and M.A. Arthur (2001) Ocean stagnation and end-Permian anoxia. *Geology*, 29, 7–10.

Iranian-Japanese Research Group (1981) The Permian and the Lower Triassic Systems in Abadeh region, central Iran. *Memoir, Fac. Sci. Kyoto Univ., ser. Geol. Mineral.*, 47(2) 61–133.

Isozaki, Y. (1994) Superanoxia across the Permo-Triassic boundary: Record in accreted deep-sea pelagic chert in Japan. In Embry, A.F., B. Beauchamp, and D.J. Glass (eds.) Pangea: Global Environments and Resources. *Mem. Canad. Soc. Petrol. Geol.* 17, 805–812.

Isozaki, Y. (1996) P-T Boundary Superanoxia and oceanic stratification in Panthalassa. In Noda, H., and K. Sashida (eds.) Prof. H. Igo Commemorative Volume on Geology and Paleontology of Japan and Southeast Asia. Gakujutu-Tosho Publ., Tokyo 29–41.

Isozaki, Y. (1997) Permo-Triassic boundary superanoxia and stratified superocean: Records from lost deep sea. *Science*, 276, 235–238.

Isozaki, Y. (2000) Plume winter: A scenario for the greatest biosphere catastrophe across the Permo-Triassic boundary. Abstr. 31th Int. Geol. Congr., 1.9–16.

Isozaki, Y. (2001) An extraterrestrial impact at the Permian-Triassic boundary? *Science*, 293, 2343a.

Isozaki, Y. (2001) Plume Winter scenario for the Permo-Triassic boundary mass extinction. *PaleoBios* 21 (Supplement no. 2) 70–71.

Isozaki, Y. (2007) Guadalupian-Lopingian boundary event in mid-Panthalassa: Correlation of accreted deep-sea chert and mid-oceanic atoll carbonate. In T. Wong (ed.), Proc. XVIth Congress of Carboniferous and Permian stratigraphy in Utrecht 2003, 21–34, Royal. Netherlands National Academy of Arts and Sciences, Amsterdam.

Isozaki, Y., H. Kawahata, and A. Ota (2007a) A unique carbon isotope record across the Guadalupian-Lopingian (Middle-Upper Permian) boundary in mid-oceanic paleoatoll carbonates: The high-productivity "Kamura event" and its collapse in mid-superocean. *Global Planetary Change*, 55, 21–38.

Isozaki, Y., S. Maruyama, and F. Furuoka (1990) Accreted oceanic material in Japan. *Tectonophysics*, 181, 179–205.

Isozaki, Y., and A. Ota (2001) Middle/Upper Permian (Maokouan/Wuchiapingian) boundary in mid-oceanic paleo-atoll limestone in Kamura and Akasaka, Japan. *Proc. Japan Acad.*, 77B, 104–109.

Isozaki, Y., N. Shimizu, J.X. Yao, Z.S. Ji, and T. Matsuda (2007b) End-Permian extinction and volcanism-induced environmental stress: The Permian-Triassic boundary interval of lower-slope facies at Chaotian, South China. *Paleogeogr. Paleoclim. Paleoecol.*, in press.

Isozaki, Y., J.X. Yao, T. Matsuda, H. Sakai, Z.S. Ji, N. Shimizu, N. Kobayashi, H. Kawahata, H. Nishi, M. Takano, and T. Kubo (2004) Stratigraphy of the Middle-Upper Permian and lowermost Triassic at Chaotian, Sichuan, China. *Proc. Japan Acad.*, 80B, 10–16.

Jin, Y.G., Y. Wang, W. Wang, Q.H. Shang, C.Q. Cao, and D.H. Erwin (2000) Pattern of marine mass extinction near the Permian-Triassic boundary in South China. *Science*, 289, 432–436.

Jin, Y.G., B.R. Wardlaw, B.F. Glenister, and G.V. Kotlyar (1997) Permian chronostratigraphic subdivisions. *Episodes*, 20, 10–15.

Jin, Y.G., J. Zhang, and Q.H. Shang (1994) Two phases of the end-Permian mass extinction. In Embry, A.F., B. Beauchamp, and D.J. Glass (eds.) Pangea: Global Environments and Resources. *Mem. Canad. Soc. Petrol. Geol.*, 17, 813–822.

Kaiho, K., Y. Kajiwara, T. Nakano, Y. Miura, H. Kawahata, K. Tazaki, M. Ueshima, Z.Q. Chen, and G.R. Shi (2001) End-Permian catastrophe by a bolide impact: Evidence of a gigantic release of sulfur from the mantle. *Geology*, 29, 815–818.

Kajiwara, Y., S. Yamakita, K. Ishida, H. Ishiga, and A. Imai (1994) Development of a largely anoxic stratified ocean and its temporary massive mixing at the Permian/Triassic boundary supported by the sulfur isotopic record. *Paleogeogr. Paleoclim. Paleoecol.*, 111, 367–379.

Kakuwa, Y. (1996) Permian-Triassic mass extinction event recorded in bedded chert sequence in southwest Japan. *Paleogeogr. Paleoclim. Paleoecol.*, 121, 35–51.

Kamo, S.L., G.K. Czamanske, Y. Amelin, V.A. Fedorenko, D.W. Davis, and V.R. Trofimov (2003) Rapid eruption of Siberian flood-volcanic rocks and evidence for coincidence with the Permian-Triassic boundary and mass extinction at 251 Ma. *Earth Planet. Sci. Lett.*, 214, 75–91.

Kato, Y., K. Nakao, and Y. Isozaki (2002) Geochemistry of Late Permian to Early Triassic pelagic cherts from southwest Japan: Implications for an oceanic redox change. *Chem. Geol.*, 182, 15–34.

Kirschvink, J.L. (1992) Late Proterozoic low-latitude global glaciation: The Snowball Earth. In Schopf, J.W., and C. Klein (eds.) The Proterozoic Biosphere, Cambridge Univ. Press, Cambridge, pp. 51–52.

Kirschvink, J.L., E.J. Gaidos, L.E. Bertani, N.J. Beukes, J. Gutzmer, L.N. Maepa, and R.E. Steinberger (2000) Paleoproterozoic Snowball Earth: Extreme climatic and geochemical global change and its biological consequences. *Proc. Natl. Acad. Sci., USA*, 97, 1400–1405.

Knoll, A.H., R.K. Bambach, D.E. Canfield, and J.P. Grotzinger (1996) Comparative Earth history and Late Permian mass extinction. *Science*, 273, 452–457.

Koeberl, C., I. Gilmour, W.U. Reimond, P. Claeys, and B. Ivanov (2002) End-Permian catastrophe by bolide impact: Evidence of a gigantic release of sulfur from the mantle: Comment and reply. *Geology*, 30, 855–856.

Koike, T. (1996) The first occurrence of Griesbachian conodonts in Japan. *Trans. Palaeont. Soc. Japan, New Series*, 181, 337–346.

Kozur, H. (1998) Some aspects of the Permian-Triassic boundary (PTB) and of the possible causes for the biotic crisis around this boundary. *Palaeogeogr. Palaeoclim. Palaeoecol.*, 143, 227–272.

Labandeira, C.C., and J.J. Sepkoski (1992) Insect diversity in the fossil record. *Science*, 261, 310–315.

Le Maitre, R.W. (1975) Volcanic rocks from EDEL no. 1 petroleum exploration well, offshore Carnavon basin, Western Australia. *J. Geol. Soc. Australia*, 22, 167–174.

Li, Z.S., L.P. Zhan, J.Y. Dai, R.G. Jin, X.F. Zhu, J.H. Zhang, H.Q. Huang, D.Y. Xu, Z. Yan, and H.M. Li (1997) Study on the Permian-Triassic Biostratigraphy and Event Stratigraphy of Northern

Sichuan and Southern Shaanxi. Geological Publishing House, Beijing (1989) 435p. (in Chinese with English abstract).

Li, Z.S., L.P. Zhan, J.X. Yao, and Y.Q. Zhou (1991) On the Permian-Triassic events in South China—probe into the end-Permian abrupt extinction and its possible causes. *Proc. Shallow Tethys (Sendai)*, 3, 371–385.

Lo, C.H., S.L. Chung, T.Y. Lee, and G.Y. Wu (2002) Age of the Emeishan flood magmatism and relations to Permian-Triassic boundary events. *Earth Planet. Sci. Lett.*, 198, 449–458.

Looy, C.V., R.J. Twitchett, D.L. Dilcher, J.H.A. van Konijinenburg-van Cittert, and H. Visscher (2001) Life in the end-Permian dead zone. *Proc. Nat. Acad. Sci. USA*, 98, 7879–7883.

Lu, Y.H. (1956) The Permian of Liangshan and its bearing on the classification and correlation of the Permian rocks of South China. *Scientia Sinica*, 5, 733–761.

MacLeod, K.G., R.M.H. Smith, P.L. Koch, and P.D. Ward (2000) Timing of mammal-like reptile extinctions across the Permian-Triassic boundary in South Africa. *Geology*, 28, 227–230.

Maruyama, S. (1994) Plume tectonics. *J. Geol. Soc. Jpn.*, 100, 24–49.

Marzoli, A., P.R. Renne, E.M. Piccirillo, M. Ernesto, G. Bellieni, and A. De Min (1999) Extensive 200 million-year-old continental flood basalts of the Central Atlantic Magmatic Province. *Science*, 284, 616–618.

Matsuo, M., K. Kubo, and Y. Isozaki (2003) Mössbauer spectroscopic study on characterization of iron in the Permian to Triassic deep-sea chert from Japan. *Hyperfine Interact. (C)*, 5, 435–438.

McArthur, J.M., and R.J. Howarth (2004) Strontium isotope stratigraphy. In Gradstein, F., J. Ogg, and A. Smith (eds.) Geologic Timescale, 2004. Cambridge Univ. Press, Cambridge, pp. 96–105.

McNutt, M.K., A.V. Judge (1990) The superswell and mantle dynamics beneath the South Pacific. *Science*, 248, 969–975.

Menning, M. (2000) Magnetostratigraphic results from the Middle Permian Type section, Guadalupe mountains, West Texas. *Permophiles*, 37, 16.

Mitchell, R.H. (1991) Kimberlites and lamproites: Primary sources of diamond. *Geosci. Canada*, 18, 1–16.

Morgan, J.P., T.J. Reston, and C.R. Ranero (2004) Contemporaneous mass extinctions, continental flood basalts, and 'impact signals': Are mantle plume-induced lithospheric gas explosions the causal link? *Earth Planet. Sci. Lett.*, 217, 263–284.

Mundil, R., K.R. Ludwig, I. Metcalf, and P. Renne (2004) Age and timing of the Permian mass extinction. *Science*, 305, 1760–1763.

Musashi, M., Y. Isozaki, T. Koike, and R. Kreulen (2001) Stable carbon isotope signature in mid-Panthalassa shallow-water carbonates across the Permo-Triassic boundary: Evidence for ^{13}C-depleted ocean. *Earth Planet. Sci. Lett.*, 196, 9–20.

Neumann, E.R., K.H. Olsen, W.S. Baldridge, and B. Sundvoll (1992) The Oslo rift: A review. *Tectonophysics*, 208, 1–18.

Nishimura, Y., T. Itaya, Y. Isozaki, and A. Kameya (1989) Depositional age and metamorphic history of 220 Ma high P/T type metamorphic rocks: An example of the Niishiki-cho area, Yamaguchi prefecture, Southwest Japan. *Mem. Geol. Soc. Jpn.*, 33, 143–166 (in Japanese with English abstract).

Ota, A., and Y. Isozaki (2006) Fusuline biotic turnover across the Guadalupian-Lopingian (Middle-Upper Permian) boundary in mid-oceanic carbonate buildups: Biostratigraphy of accreted limestone in Japan. *J. Asian Earth Sci.*, 26, 353–368.

Pakistani-Japanese Research Group Permian and Triassic Systems in the Salt Range and Surghar Range Pakistan (1985). In Nakazawa, K., and J.M. Dickins (eds.) The Tethys: Her Paleogeography and Paleobiogeography from Paleozoic to Mesozoic, Tokai Univ. Press, Tokyo, pp. 221–312.

Rabu, D., J. Le Metour, F. Bechennec, M. Beurrier, M. Villey, and C. Bourdillon-Jeudy de Grissac (1990) Sedimentary aspects of the Eo-Alpine cycle on the northeast edge of the Arabian Platform (Oman Mountains). In Robertson, A.H.F., M.P. Searle, and A.C. Ries (eds.) The Geology and Tectonics of the Oman Region. *Geol. Soc. Spec. Publ.*, 49, 49–68.

Racki, G., and P. Wignall (2005) Late Permian double-phased mass extinction and volcanism: An oceanographic perspective. In Over, D.J., J.R. Morrow, and P.B. Wignall (eds.) Understanding Late Devonian

and Permian-Triassic Biotic and Climatic Events: Towards an Integrated Approach, Cambridge Univ. Press, Cambridge, pp. 263–297.

Reichow, M.K., A.D. Saunders, R.V. White, M.S. Pringle, A.I. Al'Mukhamedov, A. Medvedev, and N. Korda (2002) $^{40}Ar/^{39}Ar$ dates from the West Siberian Basin: Siberian flood basalt province doubled. *Science*, 296, 1846–1849.

Renne, P.R., and A.R. Basu (1991) Rapid eruption of the Siberian Traps flood basalts at the Permo-Triassic boundary. *Science*, 253, 176–179.

Renne, P.R., H.J. Melosh, K. Farley, W.U. Reimold, C. Loeberl, M.R. Rampino, S.P. Kelly, and B.A. Ivanov (2004) Is Bedout an impact crater? Take 2. *Science*, 306, 610–611.

Retallack, G.J. (1999) Postapocalyptic greenhouse paleoclimate revealed by earliest Triassic paleosols in the Sydney Basin, Australia. *Geol. Soc. Amer. Bull.*, 111, 52–70.

Retallack, G.J., R.M.H. Smith, and P.D. Ward (2003) Vertebrate extinction across Permian-Triassic boundary in Karoo Basin, South Africa. *Geol Soc. Amer. Bull.*, 115, 1133–1152.

Rogers, J.J.W., and M. Santosh (2004) Continents and Supercontinents. Oxford Univ. Press, Oxford, 289p.

Saunders, A.D., R.W. England, M.K. Reichow, and R.V. White (2005) A mantle plume origin for the Siberian traps: Uplift and extension in the West Siberian basin, Russia. *Lithos*, 79, 407–424.

Schopf, T.J.M. (1974) Permo-Triassic extinctions: Relation to sea-floor spreading. *J. Geol.*, 82, 129–143.

Schubert, J.K., and D.J. Bottjer (1992) Early Triassic stromatolites as post-mass extinction disaster forms. *Geology*, 20, 883–886.

Schubert, J.K., and D.J. Bottjer (1992) Aftermath of the Permian-Triassic mass extinction event: Paleoecology of Lower Triassic carbonates in the western USA. *Paleogeogr. Paleoclim. Paleoecol.*, 116, 1–39.

Scotese, C.R., and R.P. Langford (1995) Pangea and the Paleogeography of the Permian. In Scholle, A., T.M. Peryt, and D.A. Ulmer-Scholle (eds.) The Permian of Northern Pangea, Vol. 1, Springer, Berlin, pp. 3–19.

Sepkoski, Jr., J.J. (1984) A kinetic model of Phanerozoic taxonomic diversity. III. Post-Paleozoic families and mass extinctions. *Paleobiology*, 10, 246–267.

Sorensen, H. (1974) The Alkaline Rocks, Wiley, London, 622p.

Stanley, Jr., G.D. (1988) The history of early Mesozoic reef communities: A three step process. *Palaios*, 3, 170–183.

Stanley, S.M., and X. Yang (1995) A double mass extinction at the end of the Paleozoic era. *Science*, 266, 1340–1344.

Suzuki, N., K. Ishida, Y. Shinomiya, and H. Ishiga (1998) High productivity in the earliest Triassic ocean: Black shales, southwest Japan. *Paleogeogr. Paleoclim. Paleoecol.*, 141, 53–65.

Takemura, A., M. Sakai, S. Yamakita, and 15 others (2003) Early Triassic radiolarians from Arrow Rocks in the Waipapa terrane, Northern Island, New Zealand. Abstr. InterRad, Univ. Lausanne, 64.

Thomas, B.M., R.J. Willink, K. Grice, R.J. Twitchett, R.R. Purcell, N.W. Archbold, A.D. George, S. Tye, R. Alexander, C.B. Fostre, and C.J. Barber (2004) A unique Permian-Triassic boundary section from Western Australia. *Austral. J. Earth Sci.*, 51, 423–431.

Tong, J.N., H.F. Yin, and K.X. Zhang (1999) Permian and Triassic sequence stratigraphy and sea level changes of eastern Yangtze platform. *J. China Univ. Geosci.*, 10, 161–169.

Twitchett, R.J. (1999) Paleoenvironments and faunal recovery after the end-Permian mass extinction. *Paleogeogr. Paleoclim. Paleoecol.*, 154, 27–37.

Valentine, J.W., and E.M. Moores (1970) Plate-tectonic regulation of faunal diversity and sea level: A model. *Nature*, 228, 657–659.

Veevers, J.J., and R.C. Tewali (1995) Permian-Carboniferous and Permian-Triassic magmatism in the rift zone bordering the Tethyan margin of southern Pangea. *Geology*, 23, 467–470.

Veizer, J. (2003) Isotopic evolution of seawater on geological time scales: Sedimentological perspective. In Lentz, D.R. (ed.) Geochemistry of sediments and sedimentary rocks. *Geol. Assoc. Canada, GeoText*, 4, 53–68.

Visscher, H., H. Brinkhuis, D.L. Dilcher, W.C. Elsik, Y. Eshet, C. Looy, M.R. Rampino, and A. Traverse (1996) The terminal Paleozoic fungal event: Evidence of terrestrial ecosystem destabilization and collapse. *Proc. Nat. Acad. Sci. USA*, 93, 2155–2158.

Wignall, P. (2001) Large igneous provinces and mass extinctions. *Earth-Sci. Review*, 53, 1–33.

Wignall, P., and A. Hallam (1992) Anoxia as a cause of the Permian/Triassic mass extinction: Facies evidence from northern Italy and the western United States. *Palaeogeogr. Palaeoclim. Palaeoecol.*, 93, 21–46.

Wignall, P., B. Thomas, R. Willink, and J. Watling (2004) Is Bedout an impact crater? Take 1. *Science*, 306, 609–610.

Wignall, P., and R. Twitchett (2002) Extent, duration and nature of the Permian-Triassic superanoxic event. *Geol. Soc. Amer. Spec. Pap.*, 356, 395–413.

Woods, A.D., D.J. Bottjer, M. Mutti, and J. Morrison (1999) Lower Triassic large sea-floor carbonate cements: Their origin and a mechanism for the prolonged biotic recovery from the end-Permian mass extinction. *Geology*, 27, 645–648.

Xia, W.C., N. Zhang, G.Q. Wang, and Y. Kakuwa (2004) Pelagic radiolarian and conodont biozonation in the Permo-Triassic boundary interval and correlation to the Meishan GSSP. *Micropaleontology*, 50(1), 27–44.

Xu, Y.G., S.L. Chung, B.M. Jahn, and G.Y. Wu (2001) Petrologic and geochemical constraints on the petrogenesis of Permian–Triassic Emeishan flood basalts in southwestern China. *Lithos*, 58, 145–168.

Yamakita, S., N. Kadota, T. Kato, R. Tada, S. Ogihara, E. Tajika, and Y. Hamada (1999) Confirmation of the Permian/Triassic boundary in deep-sea sedimentary rocks; earliest Triassic conodonts from black carbonaceous claystone of the Ubara section in the Tamba belt, Southwest Japan. *J. Geol. Soc. Jpn.*, 105, 895–898.

Yang, Z.M., and A. Woolley (2006) Carbonatites in China: A review. *J. Asian Earth Sci.*, 27, 559–575.

Yang, Z.Y., S.B. Wu, H.F. Yin, G.R. Xu, and K.X. Zhang (1991) Permo-Triassic events of South China. *Geol. Publ. House*, Beijing (in Chinese with English abstract).

Yin, H.F. (ed.) (1996) The Palaeozoic-Mesozoic boundary: Candidate of the Global Stratotype Section and Point of the Permian-Triassic Boundary, China Univ. Geosci. Press, Wuhan, 137p.

Yin, H.F., S.J. Huang, K.X. Zhang, H.J. Hansen, F.Q. Yang, M.H. Ding, and X.M. Bie (1993) The effect of volcanism on the Permo-Triassic mass extinction in South China. In Sweet, W.C., Z.Y. Yang, J.M. Dickins, and H.F. Yin (eds.) Permo-Triassic events in the eastern Tethys, Cambridge Univ. Press, Cambridge, pp. 146–157.

Yin, H.F., K.X. Zhang, J.N. Tong, Z.Y. Yang, and S.B. Wu (2001) The global stratotype section and point (GSSP) of the Permian-Triassic boundary. *Episodes*, 24, 102–114.

Zakharov, Y.D., G.V. Kotlyar, and A.V. Oleinikov (1995) Late Dorashamian (Late Changxingian) invertberates of the Far East and Permian to Triassic volcanism in the western Circumpacific. *Geol. Pacific Ocean*, 12, 47–60.

Zhao, D.P. (2007) Multiscale seismic tomography of mantle plumes. In Yuen, D.A., S. Maruyama, S. Karato, and B.F. Windley (eds.) Superplumes: Beyond Plate Tectonics, Springer, Dordrecht, pp. 7–30.

Zhao, J.K., J.Z. Sheng, Z.Q. Yao, X.L. Liang, C.Z. Chen, L. Rui, and Z.T. Liao (1981) The Changhsingian and Permian-Triassic boundary of South China. *Bull. Nanjing Inst. Geol. Paleont., Acad. Sinica*, 2, 1–85 (in Chinese with English abstract).

Zhou, L., and F.T. Kyte (1988) The Permian-Triassic boundary event: A geochemical study of three Chinese sections. *Earth Planet. Sci. Lett.*, 90, 411–421.

Zhou, M.F., J. Malpas, X.Y. Song, and 5 others (2002) A temporal link between the Emeishan large igneous province (SW China) and the end-Guadalupian mass extinction. *Earth Planet. Sci. Lett.*, 196, 113–122.